MoDOT

TE
5092
.M8A3
no.74-3

MacCreery

MISSOURI COOPERATIVE HIGHWAY RESEARCH PROGRAM
FINAL REPORT **74-3**

A PORTABLE SELF-MONITORING INSTRUMENT FOR LOAD HISTORY STUDIES

Property of
MoDOT TRANSPORTATION
LIBRARY

MISSOURI STATE HIGHWAY DEPARTMENT
UNIVERSITY OF MISSOURI-COLUMBIA
FEDERAL HIGHWAY ADMINISTRATION

A PORTABLE SELF-MONITORING INSTRUMENT FOR LOAD HISTORY STUDIES

STUDY 74-3

Prepared for

MISSOURI STATE HIGHWAY DEPARTMENT

by

JAMES W. BALDWIN, JR.

MARK W. WILLIAMS

DEPARTMENT OF CIVIL ENGINEERING

UNIVERSITY OF MISSOURI-COLUMBIA

COLUMBIA, MISSOURI

in cooperation with

U.S. DEPARTMENT OF TRANSPORTATION

FEDERAL HIGHWAY ADMINISTRATION

The opinions, findings, and conclusions expressed in this publication are not necessarily those of the Federal Highway Administration

ABSTRACT

Development and operation of a portable instrument for recording strain events in bridges under field service conditions are described. The instrument consists of a transducer, which is clamped to the flange of a bridge by four allen screws, a set of mechanical counters driven by electronic logic circuitry, a battery pack, and a tamper-proof enclosure. As much as eighty days continuous operation can be realized before batteries must be serviced.

Each counter is incremented every time the strain reaches the triggering level selected for that counter. Triggering levels are selected so as to be distributed over a range slightly greater than the strain range expected in the bridge. For the usual case where the triggering levels are all in the elastic range, a simple hand calculation will produce a stress histogram from the counter readings.

The theory and a procedure for predicting bridge life from the collected data are also presented. Results of a short field test indicate that the instrument provides a practical and economical means for relatively unskilled personnel to collect stress history data.

ACKNOWLEDGEMENTS

The design and development program reported herein was conducted by the Engineering Experiment Station of the University of Missouri-Columbia under the sponsorship of the Missouri State Highway Commission in cooperation with the Federal Highway Administration of the U.S. Department of Transportation. Sincere appreciation is expressed to these organizations for the financial support of this work and additionally to those individuals of the bridge divisions who contributed guidance and review throughout the study.

All analytical work and the design of the transducer was carried by Mr. Mark W. Williams, Graduate Research Assistant in Civil Engineering. Design and development of the electronic circuitry was carried out in the Instrumentation Design Group of the Engineering Experiment Station by Messrs. John McCurdy and John Uhlig under the supervision of Associate Professor B. W. Sherman. Fabrication of the transducer and tamper-proof enclosure was carried out by Mr. Bill Ballard of the Civil Engineering Shop. The entire project was under the general supervision of Professor James W. Baldwin, Jr., Professor of Civil Engineering

TABLE OF CONTENTS

	Page
ACKNOWLEDGEMENTS	ii
LIST OF TABLES	v
LIST OF FIGURES	vi
Chapter	
1. INTRODUCTION	1
1.1 PROBLEM STATEMENT	1
1.2 PROPOSED INSTRUMENTATION.	1
1.3 SIGNIFICANCE OF WORK.	2
2. THEORY OF OPERATION	4
2.1 FATIGUE CONSIDERATIONS	4
2.2 APPLICATION OF THE HISTOGRAM	6
2.2.1 Example of Stress Range Determination.	11
2.3 CUMULATIVE DAMAGE IN FATIGUE	13
2.4 SELECTION OF STRESS LEVELS.	15
3. INSTRUMENT DESIGN	21
3.1 THE STRAIN TRANSDUCER	21
3.2 THE RECORDER	24
3.3 THE POWER SUPPLY	32
3.4 TOTAL INSTRUMENT PACKAGE	34
4. DATA ANALYSIS	36
4.1 EXAMPLE OF FATIGUE ANALYSIS	36
4.2 CRITICAL STRESSES	39

Chapter Page

4.3 INFLUENCE ENVELOPES FOR MULTI-SPAN BRIDGES 40

5. INSTALLATION AND OPERATION 48

5.1 GENERAL. 48

5.2 INSTALLATION OF COMPONENTS 48

5.2.1 The Strain Transducer and Housing Assembly. 48

5.2.2 The Recorder Housing Assembly . 49

5.3 INSTRUMENT OPERATION 54

6. FIELD TEST 59

7. SUMMARY 67

REFERENCES 69

APPENDIX A. NOMENCLATURE 71

APPENDIX B. PARTS LIST 73

APPENDIX C. CIRCUIT DIAGRAMS 79

LIST OF TABLES

Table		Page
4-1.	Sample Calculations for Fatigue Analysis . . .	36
6-1.	Stress History - Dec. 4 - Dec. 19	62
6-2.	Stress History - Dec. 19 - Dec. 31	62

LIST OF FIGURES

Figure		Page
2-1.	Typical Stress or Strain Trace	5
2-2.	Stress Range Histogram - Douglas (5)	7
2-3.	Simulated Strain Trace and Associated Counting Levels	8
2-4.	Simulated Strain Trace for an Actual Loading Cycle	10
2-5.	Sample Determination of Stress Ranges	12
2-6.	Stress Range Histogram and Cumulative Exceedence Curve	14
2-7.	Fatigue Curve for Beams with End-welded Cover Plates - Fisher (13)	16
2-8.	Cumulative Fatigue Damage	17
2-9.	Sample Damage Curve	18
3-1.	The Prototype Strain Transducer	22
3-2.	Cut-A-Way of Prototype Transducer	23
3-3.	Typical Counter Circuit Diagram	26
3-4.	Signal Conditioning Schematic	28
3-5.	Counter Circuit Schematic	29
4-1.	Cumulative Exceedence Curve for Sample Extrapolation	35
4-2.	Axle Spacing and Weight Distribution for Truck Types I, II and III	40
4-3.	Three-span Continuous Bridge Profile	42
4-4.	Maximum Moment Range Envelope for Sample 3-Span Bridge (Left Endspan)	43
5-1A.	Strain Transducer with Spacer Bar	48
5-1B.	Transducer Mounting Block	48
5-2.	Recorder Housing Assembly	49

Figure		Page
5-3.	Recorder Housing Clamping Screws	49
5-4.	Instrument Rack	50
5-5.	Positioning Recorder	50
5-6.	Installing Batteries	51
5-7.	Cable Connection	51
5-8A.	Transducer Zero Adjustment	53
5-8B.	Checking Transducer Zero	53
5-9A.	Setting Triggering Levels	54
5-9B.	Reseting Counter	54
5-10A.	Waterproof Recorder Cover	55
5-10B.	Housing Cover	55
6-1.	Field Test Layout	60
6-2.	Field Installation	61
6-3.	Stress Ranges Dec. 4-19	64
6-4.	Stress Ranges Dec. 19-31	65

CHAPTER 1

INTRODUCTION

1.1 PROBLEM STATEMENT

In recent years, limited field studies (1-10) have indicated that actual service stresses in highway bridges may be far below the calculated maximum stresses for which bridges are designed; however, considerably more data is needed before conclusions may be drawn as to whether revisions to present design criteria may be possible or necessary.

At the present, field studies of service stresses require a substantial amount of expensive equipment and skilled research personnel. Unfortunately, these studies have been limited, by expense, to observations of a relatively small number of bridges for relatively short periods of time. Clearly, there is a need for a new, more economical means of data collection that will allow studies to be performed on a much wider variety of bridges for much longer periods of time.

1.2 PROPOSED INSTRUMENTATION

This report presents the design, theory of operation and application of a lightweight, portable, self-monitoring instrument for load history studies. The instrument is a compact, battery-powered electronic device which can be easily attached to a steel bridge, by relatively unskilled

personnel, and left in place indefinitely, subject only to battery recharging approximately once a month. Basically, the unit consists of three main components: (1) the strain transducer, (2) the recorder, and (3) the battery pack. The strain transducer monitors the strain events taking place due to the passage of vehicles across the bridge.

The recorder, consisting of a series of counters (each corresponding to a pre-set stress level), monitors the output signal from the strain transducer. A particular counter is advanced when the output of the strain transducer exceeds the pre-set stress level corresponding to that counter. The counters, and their related circuitry, are designed such that any number of counting units can be built into the system. The recorder and transducer are powered by a battery pack that supplies 24 VDC to the complete system. In addition to the instrumentation, a simple analytical procedure has been developed for interpretation of the results in terms of a stress range histogram or in terms of bridge fatigue life.

1.3 SIGNIFICANCE OF WORK

The availability of this instrument will make it possible for highway department personnel to collect load history information from a variety of bridges at a relatively low cost. In addition to determining the actual service stresses in bridges, the instrument could also be used to observe: (1) the long-range trends of traffic volume, (2) the effectiveness of weigh stations, (3) the effects of

changes in legal weight limits, and (4) the presence of overweight vehicles, in areas where there are no weight stations or at times when such stations are closed.

CHAPTER 2

THEORY OF OPERATION

2.1 FATIGUE CONSIDERATIONS

Most recent load history studies have incorporated a fatigue analysis on the basis of collected data. Such an analysis requires knowledge concerning the behavior of the particular material under fatigue loading and the important parameters governing this behavior.

Fisher (13) has conducted in-depth studies on fatigue, with respect to weldments on steel beams, and concluded from these studies that stress range alone is the dominant variable in a fatigue analysis for structural steel bridges. From the data accumulated, fatigue curves for a variety of structural details have been developed. These curves are represented by a linear log-log relationship between the stress range, Sr, and cycles to failure, N.

The stress range, as defined by Fisher and others (5, 12), is taken as the algebraic difference between the maximum and minimum stress values from each loading cycle. A typical stress or strain trace is shown in Figure 2-1. The intermediate peaks and valleys shown in the figure are due to particular axle spacings and vibrations.

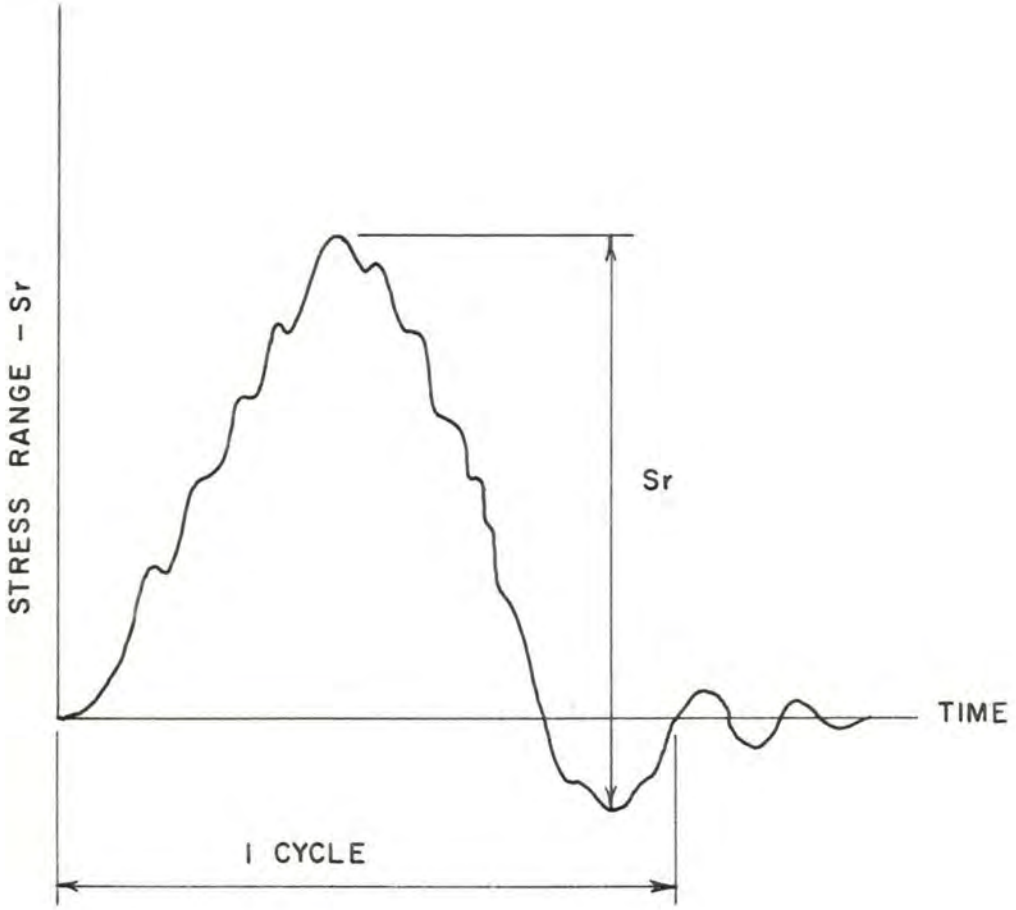

FIGURE 2-1 TYPICAL STRESS OR STRAIN TRACE

2.2 APPLICATION OF THE HISTOGRAM

Load histories are generally collected as an analog recording which is subsequently processed through an analog-to-digital converter. Then, from the digital record, the maximum and minimum stress values are determined and combined to obtain the stress range. The data are subsequently grouped in discrete intervals from which the frequency of occurrences of stress ranges within each interval may be determined. The result of this procedure presented graphically is known as the stress-range-frequency histogram. An example of such a histogram is given in Figure 2-2.

Assume now that a series of counters is introduced in lieu of a sophisticated data acquisition system. Each counter is incremented when the stress level reaches a pre-selected value as indicated in Figure 2-3. A given counter cannot be incremented again until the stress level has gone below some pre-selected value near zero. For the single cycle shown, counters 1-4 are each incremented once. Counters 5 and 6 are not incremented since the analog signal representing the strain trace does not exceed their corresponding stress levels.

If it is assumed that a similar sequence of counting occurs, as above, for each trace caused by a passing vehicle then, for the length of the test period associated with a particular bridge study, each counter total, C_i, reflects the number of times that its associated stress level,

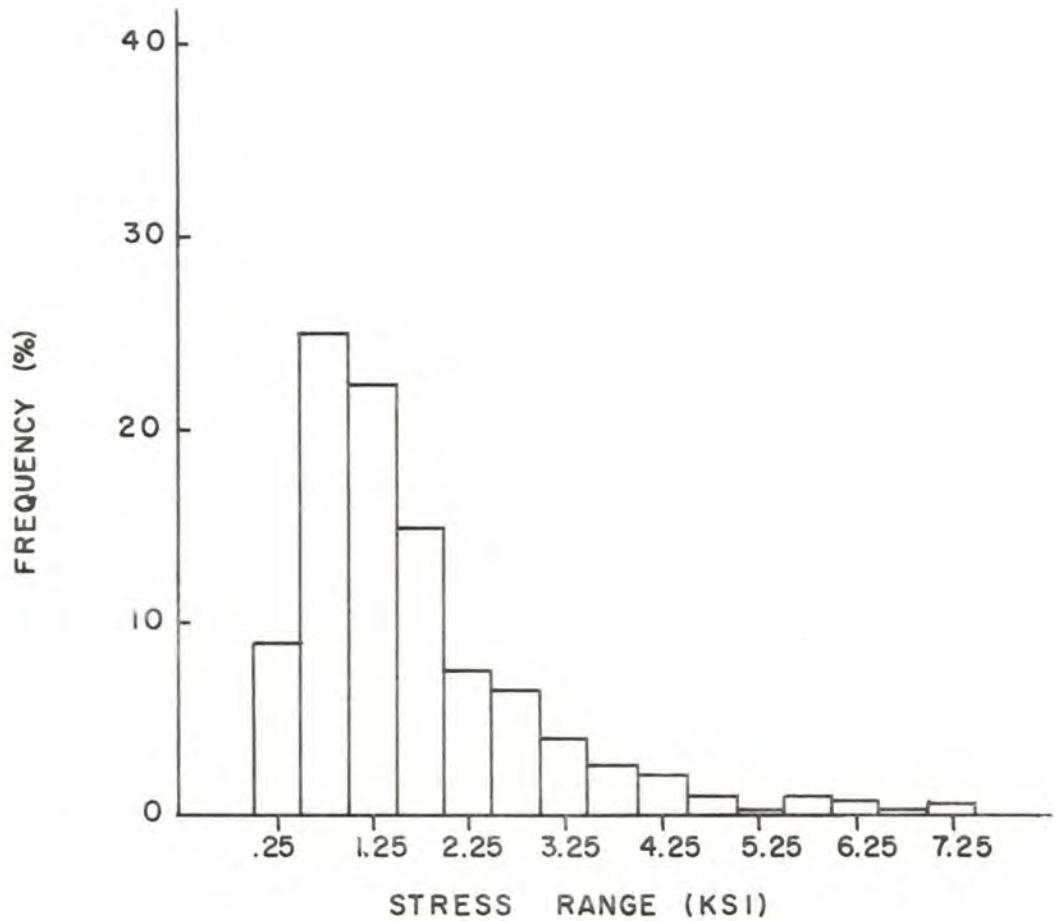

FIGURE 2-2 STRESS RANGE HISTOGRAM - DOUGLAS (5)

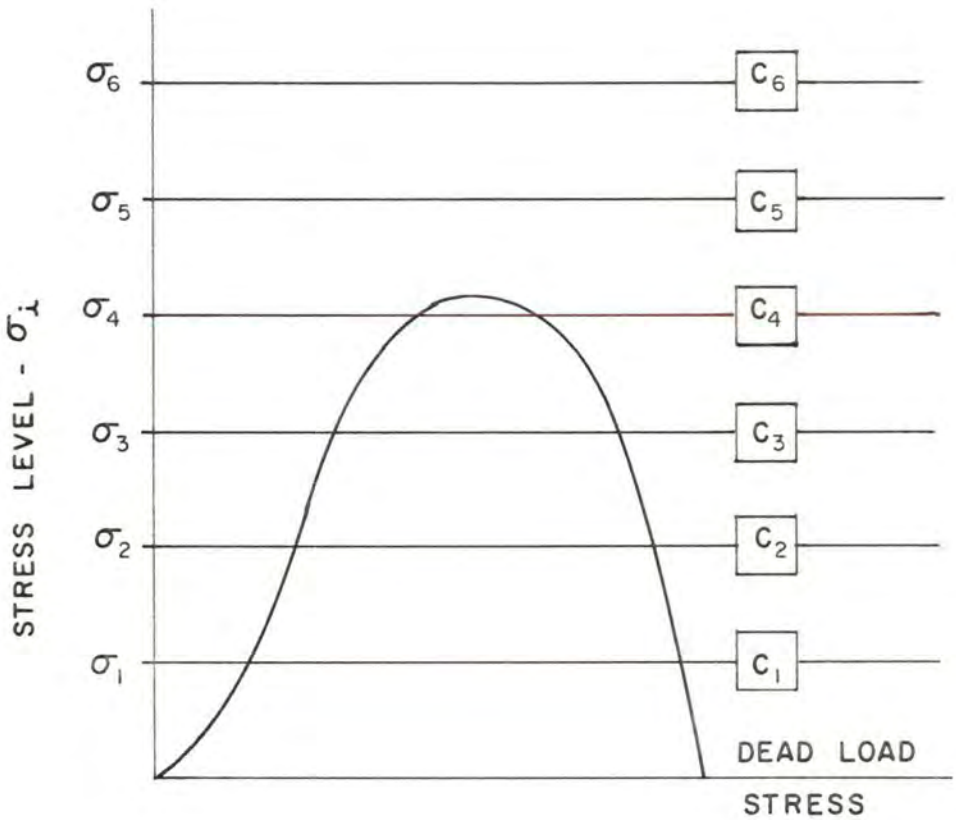

FIGURE 2-3 SIMULATED STRAIN TRACE AND ASSOCIATED COUNTING LEVELS

σ_i, was exceeded.[1]

Furthermore, if no negative portion of the strain trace exists, as in Figure 2-3, then

$$\sigma_i = Sr_i \qquad (i = 1,2,\ldots,m),$$

and

$$C_i = Cr_i$$

where m is the number of active counters, and Cr_i is the number of times that stress range Sr_i has been exceeded. Clearly, C_1, is equal to the total number of significant events that occurred over the test period.

Consider now that a negative portion of the strain trace does occur, which it would in a multi-span bridge structure. Figure 2-4 represents a typical loading cycle where each counter associated with a negative stress level is incremented in the same manner as previously indicated for positive counters. Therefore, it remains to combine the stress levels (Fig. 2-4) by some method in order to obtain the necessary stress ranges for subsequent analyses.

In general, it may be assumed that a higher positive stress occurrence results in an algebraically lower negative stress occurrence. Therefore, the stress levels indicated in Figure 2-4 may be associated to form stress ranges by a comparative analysis of the cumulative number of exceedences,

---

[1]The subscript i is used to relate particular counter readings to associated stress levels and is also used to relate various other parameters to associated stress ranges.

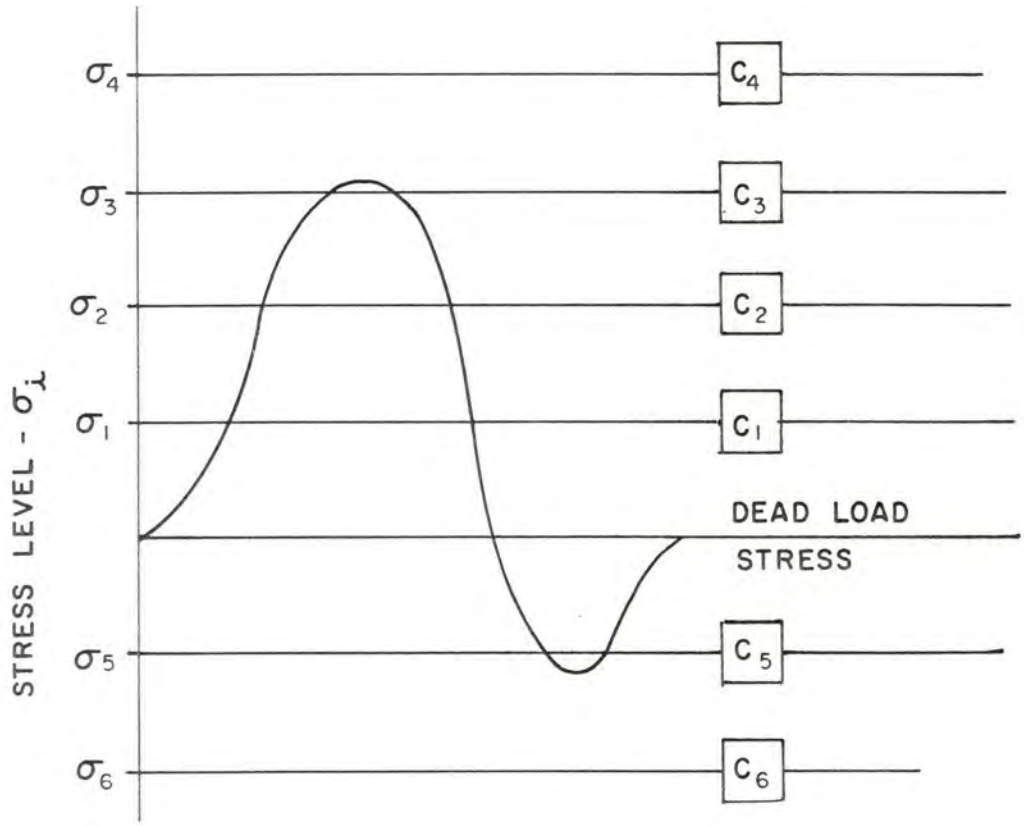

FIGURE 2-4 SIMULATED STRAIN TRACE FOR AN ACTUAL LOADING CYCLE.

C_i and C_j, of positive and negative stress levels, σ_i and σ_j, respectively. This procedure is initiated at the extreme positive and negative stress levels (in this case σ_4 and σ_6). By a process of elimination, the cumulative number of exceedences for each possible stress range is determined. The following numerical example will serve to illustrate the procedure.

2.2.1 Example of Stress Range Determination

Consider the stress levels and cumulative counter totals shown in Figure 2-5. To start, the extreme counter totals, C_4 and C_6, are compared. The lower total, C_4, is then equal to the cumulative number of exceedences, Cr_1, of stress range, Sr_1, where Sr_1 is equal to the algebraic difference of σ_4 and σ_6. The higher value, in this case C_6, is retained and compared to the next descending counter, C_3. Since C_3 is less than C_6, $C_3 = Cr_2$, where Sr_2 is equal to the algebraic difference of σ_3 and σ_6. This procedure is carried on until all counter totals have been considered.

Note that if C_3 had been equal to C_6, then, $Cr_2 = C_3 = C_6$. In this case, no counter total is retained, and the next comparison is made between C_2 and C_5. This procedure is followed whenever two counter totals are compared and found to be equal.

The final stress ranges and the cumulative number of exceedences for each range are also shown in Figure 2-5. The stress range histogram for the data in Figure 2-5 is

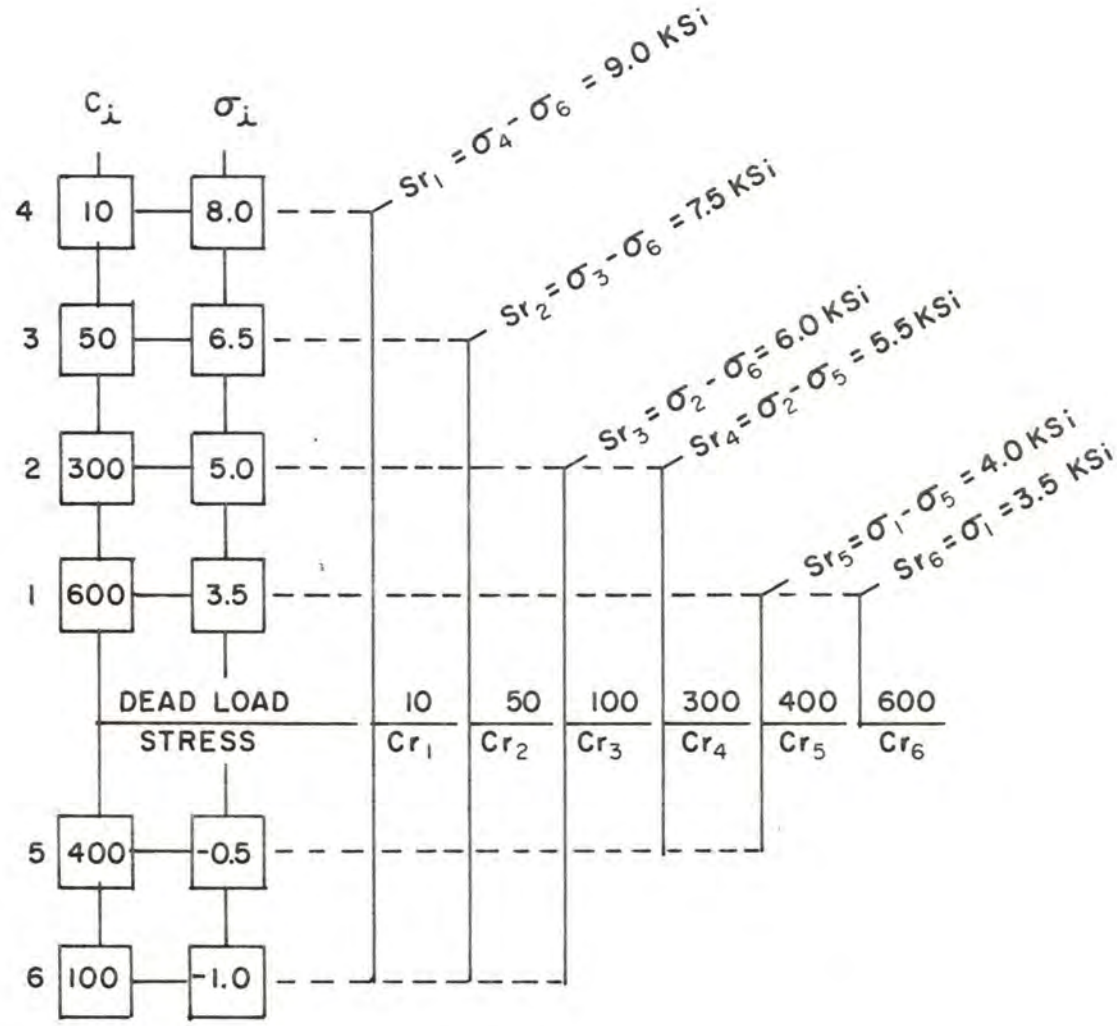

FIGURE 2-5 SAMPLE DETERMINATION OF STRESS RANGES.

shown in Figure 2-6. The arrow to the right of Sr_1 indicates that the upper bound of the histogram is unknown. This point may be estimated by superimposing and extrapolating the cumulative exceedence curve (dashed line). If desired, however, this point might be neglected since the percent frequency of occurrence is generally quite small in that region.

2.3 CUMULATIVE DAMAGE IN FATIGUE

In addition to determining the stress range histogram, it may be desirable to estimate the long-range effects that fatigue may have on the useable life of a bridge. Miner's cumulative damage theory (11) is commonly used as a basis for fatigue analysis. It will be used here, for simplicity, to illustrate how data similar to that shown in Figure 2-6 may be used to determine the fatigue damage incurred by a bridge due to the random loading cycles encountered under service conditions. Damage is defined as the fractional part of the total life that is expended during any given number of cycles.

According to Miner's theory, the total damage is independent of the order of application of random loading cycles. Based on this assumption, the total damage is given by

$$\text{Damage} = \sum \frac{n_\ell}{N_\ell} \leq 1.0 \text{ (failure)}$$

where n_ℓ is equal to the actual number of cycles at stress range, Sr_ℓ, and N_ℓ is equal to the number of cycles to failure at Sr_ℓ.

The number of cycles to failure, N, should be determined from a fatigue curve that is based on experimental data

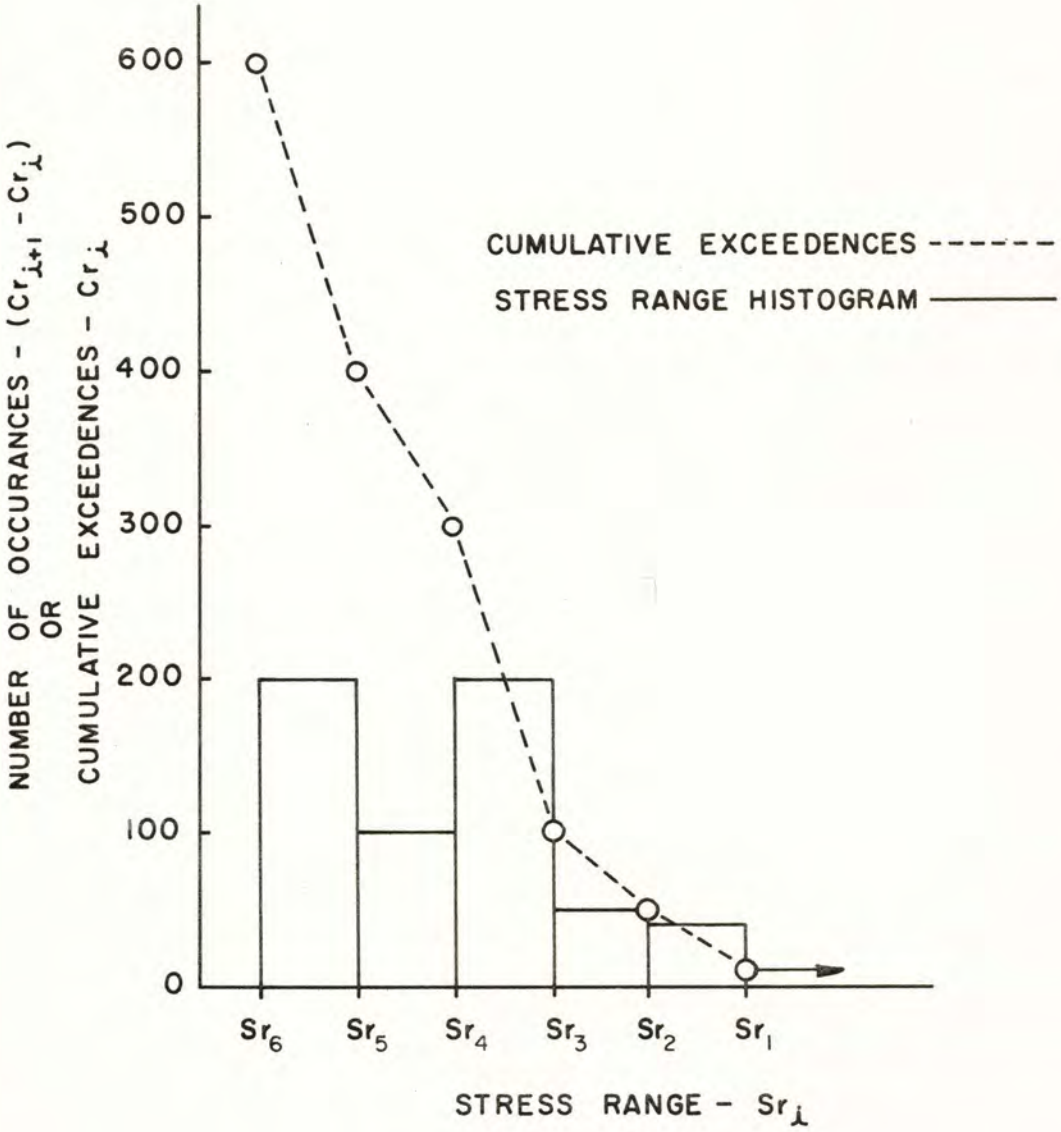

FIGURE 2-6 STRESS RANGE HISTOGRAM AND CUMULATIVE EXCEEDENCE CURVE.

from structural details that are the same as, or similar to, the actual detail or details under consideration. A fatigue curve, developed by Fisher, for beams with end-welded cover plates is shown in Figure 2-7.

Assume now that a given number of cycles, A_i, occur at stress ranges somewhere between Sr_i and Sr_{i+1}, where A_i is equal to the difference between the cumulative number of exceedences, Cr_i and Cr_{i+1}, of stress ranges, Sr_i and Sr_{i+1}, respectively (Fig. 2-8). The damage due to the kth cycle at some stress range between Sr_i and Sr_{i+1} is indicated by the cross-hatched area in Figure 2-8. Furthermore, if A_i is very large and assumed to be uniformly distributed within the interval, $Sr_{i+1} < Sr_i$, then the total damage is equal to the area bounded by CDAB and the smooth curve BFC. For relatively small stress range intervals, however, a trapezoidal approximation of the curve (dashed line) may be used which gives

$$\text{Damage} = \frac{A_i}{2} \left(\frac{1}{N_i} + \frac{1}{N_{i+1}}\right) \qquad (2\text{-}1)$$

A sample damage curve developed from data in Figure 2-5 and Figure 2-7 is shown in Figure 2-9.

2.4 SELECTION OF STRESS LEVELS

Once again, consider a series of counters as in Section 2.2. At the outset of a particular bridge study it is necessary to make an initial selection of stresses at which to set the adjustable counting levels. Although the theory

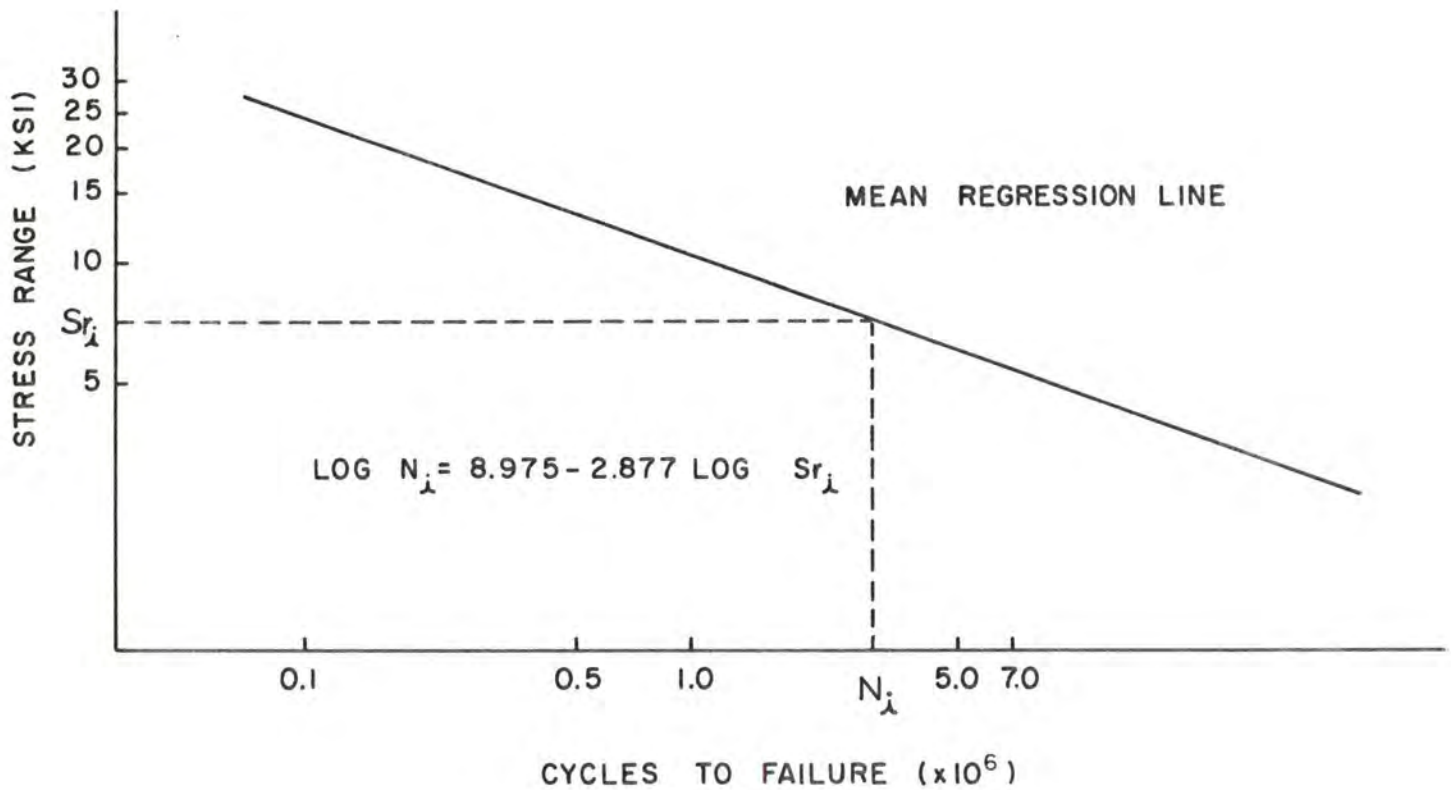

FIGURE 2-7 FATIGUE CURVE FOR BEAMS WITH END-WELDED COVER PLATES - FISHER (13).

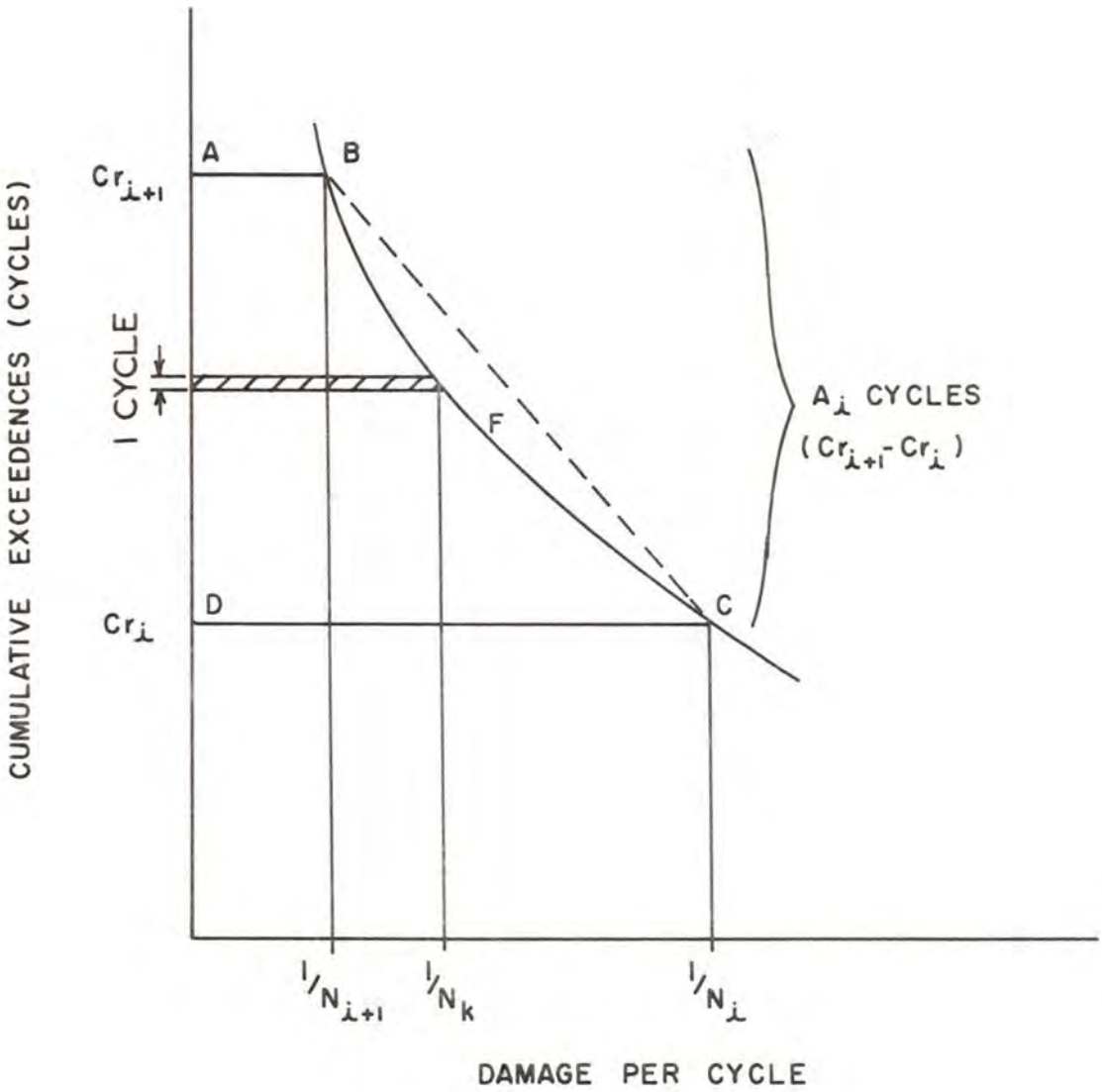

FIGURE 2-8 CUMULATIVE FATIGUE DAMAGE

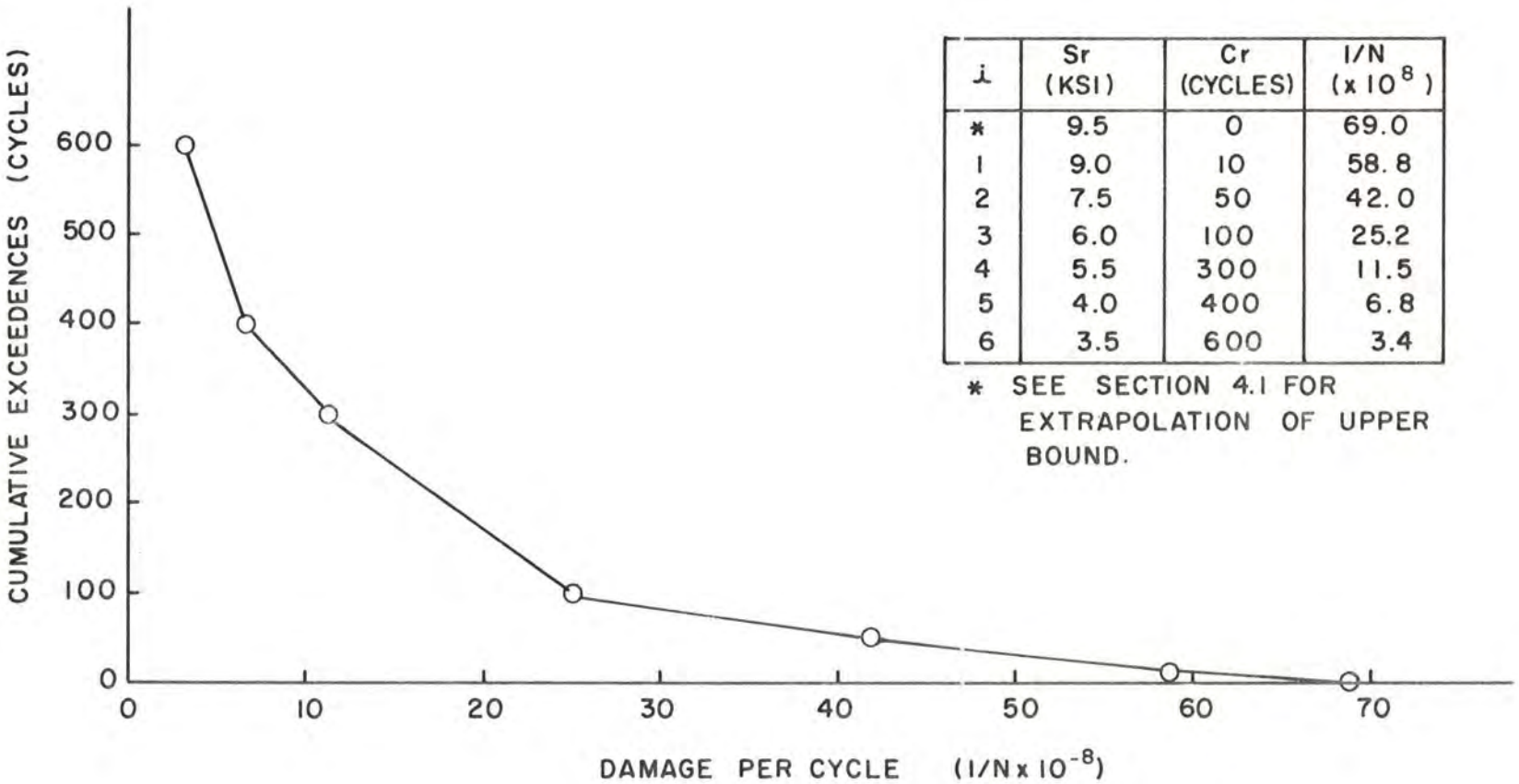

i	Sr (KSI)	Cr (CYCLES)	1/N (x 10^8)
*	9.5	0	69.0
1	9.0	10	58.8
2	7.5	50	42.0
3	6.0	100	25.2
4	5.5	300	11.5
5	4.0	400	6.8
6	3.5	600	3.4

* SEE SECTION 4.1 FOR EXTRAPOLATION OF UPPER BOUND.

FIGURE 2-9 SAMPLE DAMAGE CURVE.

of operation applies to an arbitrary selection of stress levels, the speed and accuracy with which results may be obtained can be increased somewhat by a judicious selection.

It is therefore suggested that the maximum positive and negative stress levels should be estimated by some means. The use of maximum moment envelopes may provide a relatively simple method for accomplishing this purpose if they have been previously determined (see Chapter 4). Otherwise, any applicable method is suitable.

When the desired maximum levels have been determined, one adjustable monitor should then be set slightly below each of these levels. (The term "monitor" refers to the stress level at which a particular counter is incremented). If it is assumed that a fatigue limit does exist, the remaining positive monitors should then be spaced in even intervals between the maximum expected stress and the fatigue limit. The remaining negative monitors should then be spaced in even intervals between the maximum and minimum negative stress levels, $\sigma_{(max)j}$ and $\sigma_{(min)j}$, such that the proportional relationship

$$\frac{\sigma_{(min)j}}{\text{Fatigue Limit}} = \frac{\sigma_{(max)j}}{\sigma_{(max)i}} \quad \text{is satisfied.}$$

If no fatigue limit exists, then both positive and negative threshold levels may be set somewhat arbitrarily. They should, however, be set proportionally, as above, and high enough so that noise in the system does not cause counters to be incremented.

It may be desirable, periodically, to observe data being recorded by the instrument since the initial maximum stress estimates may not be quite correct. In order to be reasonably sure that all cycles at the highest stress range are accounted for, $C_{i(max)}$ and $C_{j(max)}$ should not exceed approximately 1% of $C_{i(min)}$ and $C_{j(min)}$, respectively.

The prototype instrument is presently equipped with circuitry for ten counting levels. Each may be set to monitor either positive or negative levels. In addition, the ratio of the number of positive counters to negative counters should be approximately equal to the ratio of the maximum estimated positive and negative stress levels.

CHAPTER 3

INSTRUMENT DESIGN

3.1 THE STRAIN TRANSDUCER

The strain transducer is a sensing device used to produce an analog voltage signal proportional to the strain in a structural steel bridge girder.

The sensing element used in this study is a Hewlett-Packard Model 24DCDT-100. This type of sensing element is a direct current differential transformer (DCDT) requiring 24VDC excitation and provides an output signal of ±10VDC over a displacement range of ±0.10 inches. The actual strain is therefore the displacement divided by the gage length.

The gage length of the prototype transducer is 40 inches which provides an output signal of approximately 4mv/micro-strain without amplification. The prototype transducer is shown in Figure 3-1 with the DCDT located internally in the righthand mounting block. A sectioned view of the transducer and other internal parts is illustrated in Figure 3-2.

When the transducer is attached to a bridge girder, the gage rod is supported at its midpoint by a teflon bearing surface mounted on a steel angle which clamps on the bottom flange of the girder. This support minimizes vibration of

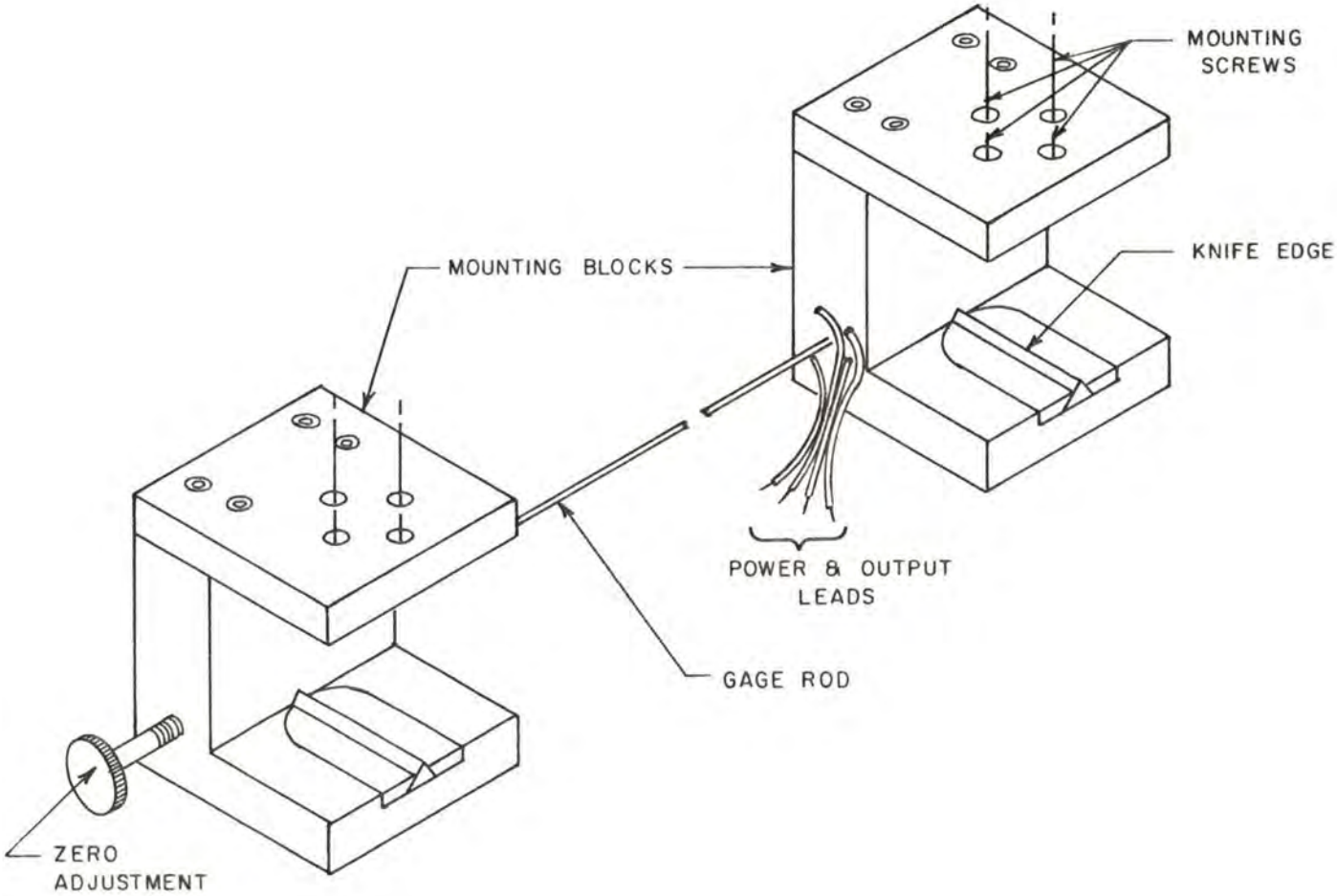

FIGURE 3-1 THE PROTOTYPE STRAIN TRANSDUCER

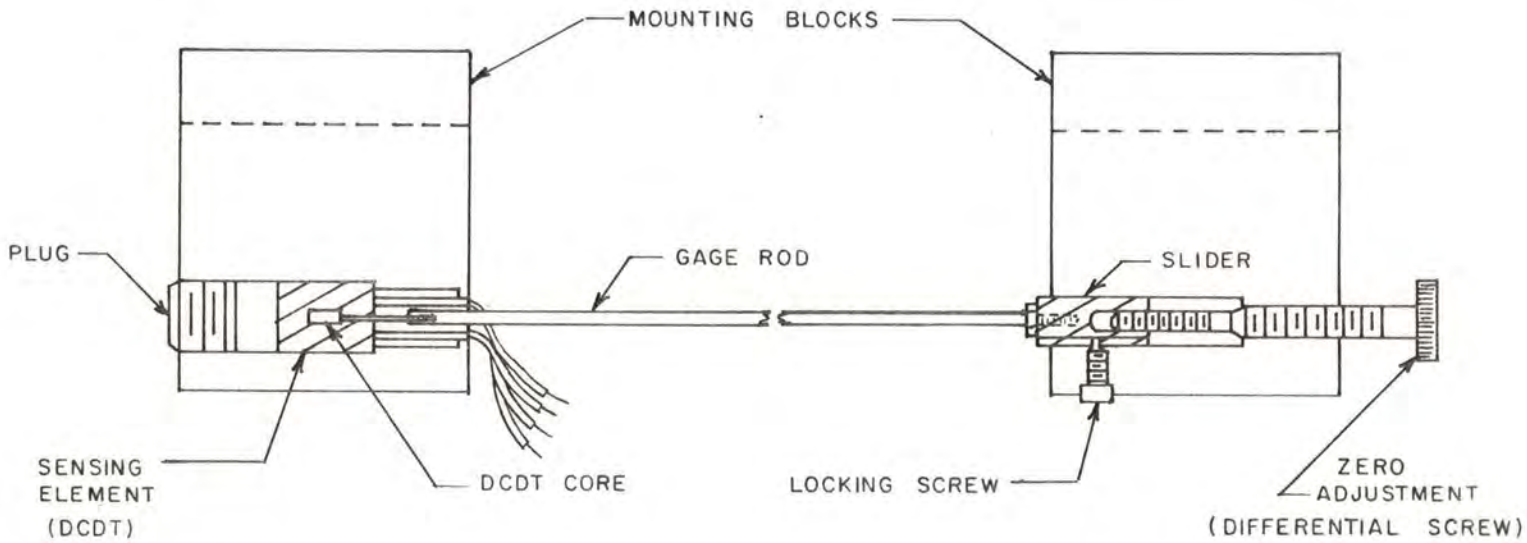

FIGURE 3-2 CUT-A-WAY OF PROTOTYPE TRANSDUCER

the rod, due to wind and other dynamic loads, and helps the rod conform to the curvature of the girder.

Further information regarding the strain transducer is provided in Chapter 5 - Installation and Operation.

A relatively small modification to the recorder would permit the use of an electric resistance strain gage as a transducer. This would greatly reduce the gage length over which the strain is measured and cut the power requirements in half. However, one objective of this particular design was to produce a fairly rugged re-usable transducer that could be installed in the field without special tools or skill.

3.2 THE RECORDER

The recorder is an electronic package designed to receive and monitor the output signal from the strain transducer. Inside the recorder, a series of counters, each triggered at an adjustable stress or strain level, record stress events as they occur.

Two models of the counter were designed and built. Model I consists of six counters each with a separately adjustable triggering level and re-arming level. Model II consists of ten counters each with a separately adjustable triggering level, but all counters are re-armed simultaneously when the input signal crosses the zero line. Model II has some additional features which improve its performance and reduce the manufacturing cost.

3.2.2 Model I

A circuit diagram for a single counter of the model I recorder is shown in Figure 3-3. The circuit consists of four main sections: (1) the level detector (IC_1- IC_2), (2) the latching circuit (IC_3- IC_4), (3) the driver trigger (IC_5-IC_6), and (4) the counter driver.

Voltage comparator IC_1 is DC coupled to the transducer output on both the positive and negative inputs through $R_1$and R_3. Capacitor C_2 filters the AC portion of the transducer output from the negative input to the comparator. The DC drift of the datum level is therefore cancelled when the total signal is applied to the positive comparator input. The activation level of IC_1 is set by $R_5(V_s)$ which corresponds to some pre-selected stress level. Voltage comparator IC_2 functions identically to IC_1, except it acts as an inverting comparator to re-arm the latching circuit. The latching circuit prevents the counter from functioning until the output signal from the transducer drops below some preselected stress level set by $R_{10}(V_R)$. The latching circuit fires a "one-shot" pulse from the driver (Q_1) to insure that the mechanical counter is incremented. As a safeguard, D_1 prevents damage to Q_1 due to back voltage from the counter coil.

3.2.2 Model II

During testing of the Model I recorder it was decided that a number of improvements could be made in the circuitry which would both improve the performance and cut the cost of manufacture. In addition it appeared that individual re-arming

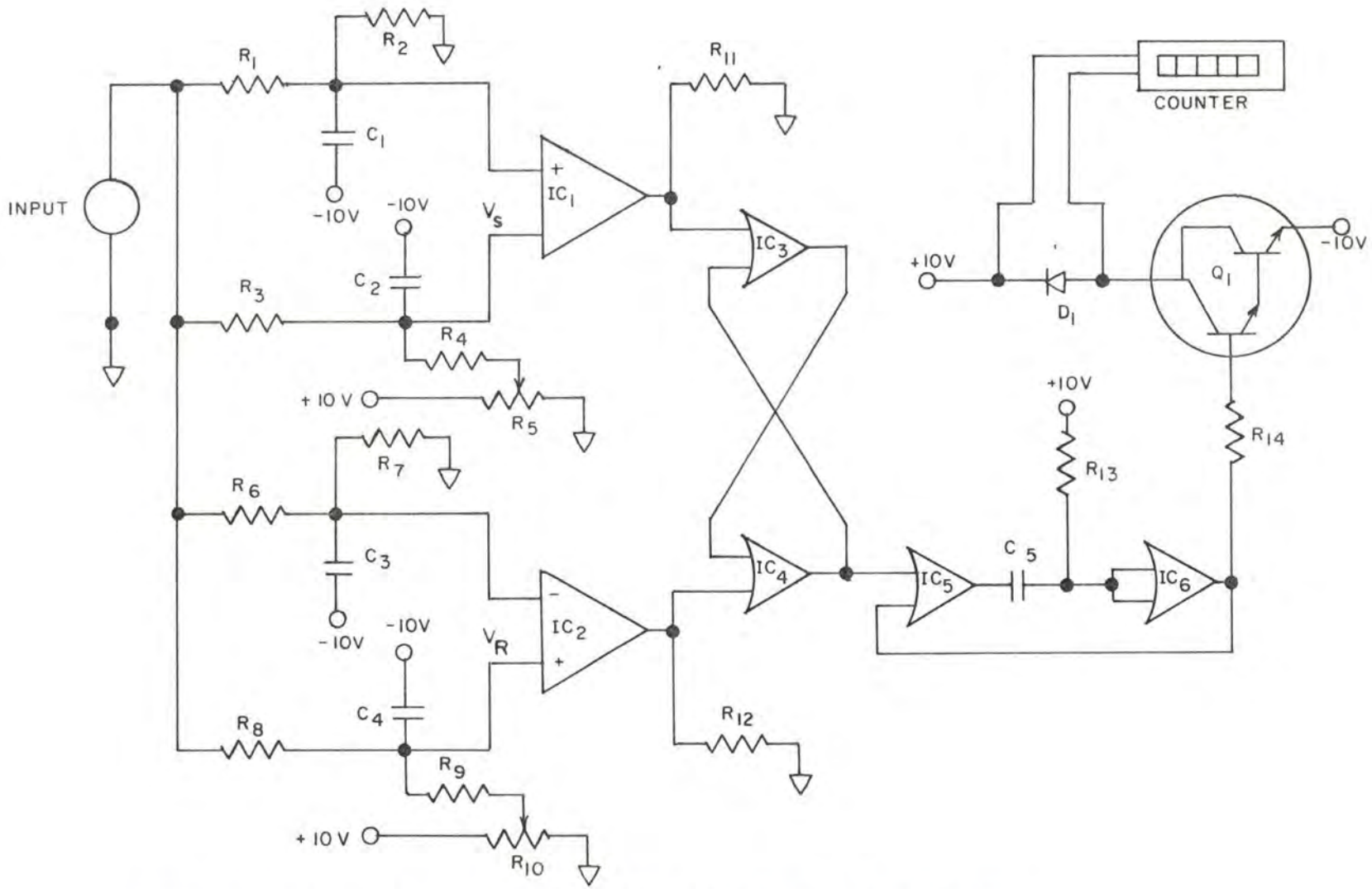

FIGURE 3-3 TYPICAL COUNTER CIRCUIT DIAGRAM

controls for each counter were not as useful as extra counters would be. Finally, under very heavy slow moving traffic the drift compensation circuitry of the Model I was not adequate. In order to incorporate all the improvements and modifications as efficiently as possible the recorder was completely redesigned and a Model II was fabricated. Schematic diagrams of the circuitry are shown in Figures 3-4 and 3-5.

IC1 is an FET-input operational amplifier connected as a voltage follower to provide a high input impedance buffer. Operational amplifier IC2, also an FET-input op-amp voltage follower, follows the dc-component of the input, provided by low pass filter R2-C1. The dc component is subtracted from the buffered transducer output by X1 precision difference amplifier IC3, providing only the ac component of the transducer signal at the low-impedance output of IC3.

Since a slow-moving truck may take as long as 30 seconds to cross a bridge span, the time constant of R2-C1 is necessarily long, R2C1 = (100 megohms) (24 ufd) = 2400 seconds. Three time constants, 7200 sec = 2.0 hours, must elapse in order for the voltage on C1 to come within 95% of the dc voltage at the input. Both in the field and on the laboratory bench, two hours is an inconveniently long time to wait for the counter to settle after application of power. Any abrupt change of the dc input level would require another two hours settling, which is undesirable from testing and calibration aspects.

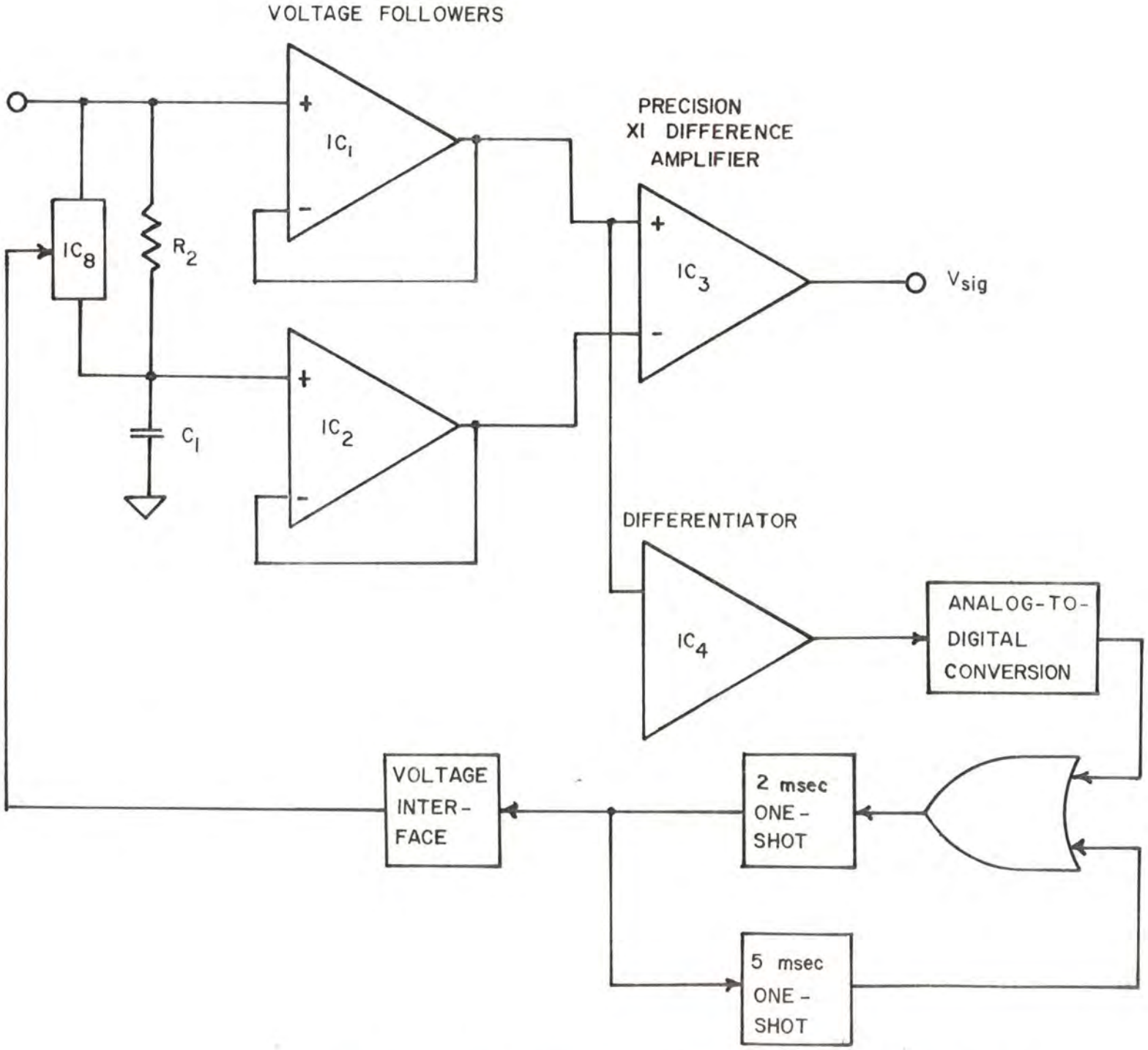

FIGURE 3-4 SIGNAL CONDITIONING SCHEMATIC

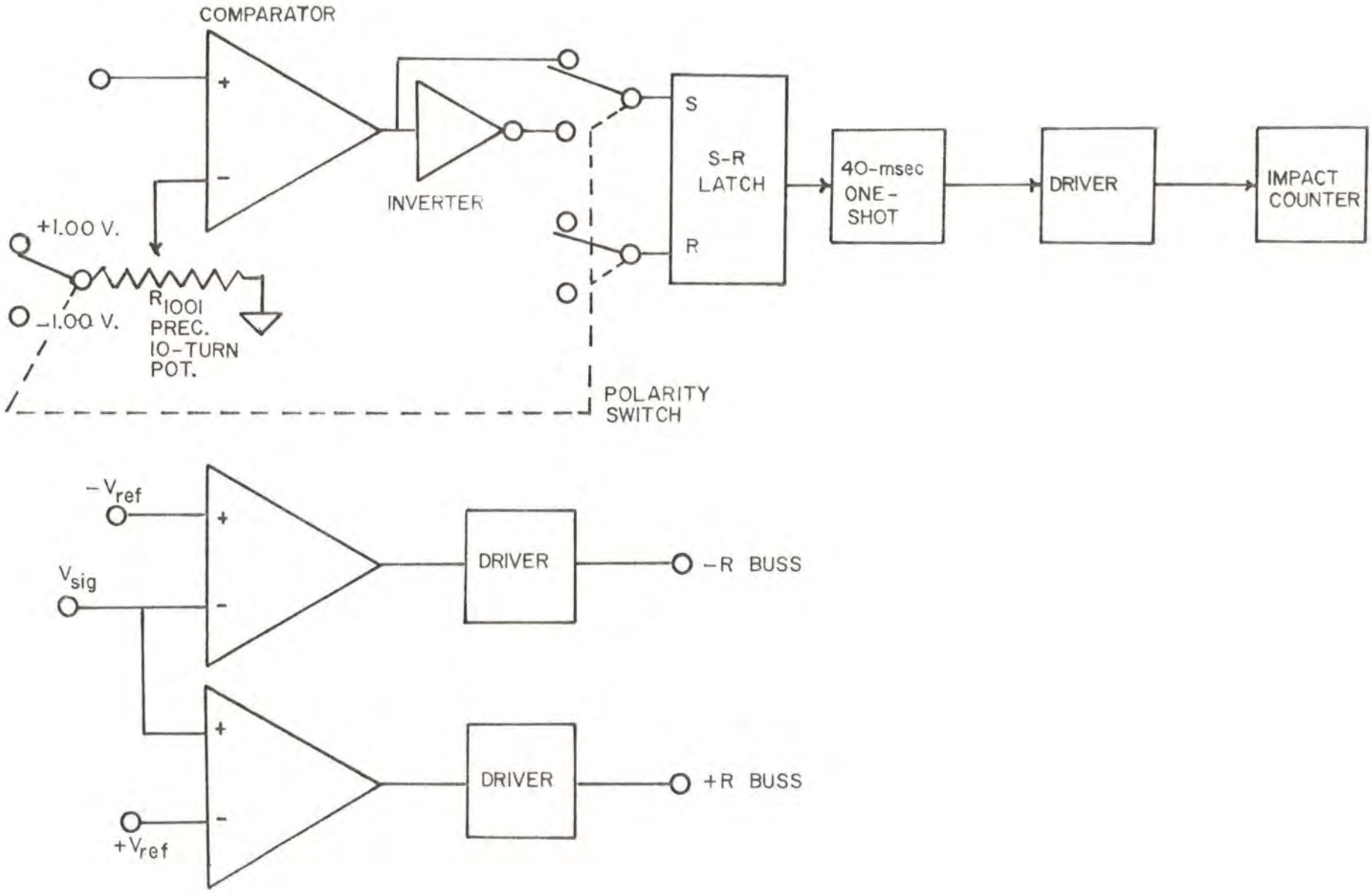

FIGURE 3-5 COUNTER CIRCUIT SCHEMATIC

While normal field conditions will yield slow changes in the ambient dc level, several abnormal conditions could cause a rapid change, relative to the two-hour settling time, in the ambient dc level. Traffic which stops on the bridge and subsequently moves off the bridge in a relatively short period of time would produce such a change.

To overcome the problem of this error voltage buildup, the following approach was used.

1.) Detect the absence of an a.c. signal.

2.) When no a.c. signal is present, short R2 with a much much smaller resistance in order to reduce the R2-C1 time constant.

3.) Cycle the shorting of R2 so that R2-C1 filtering can be resumed before affecting the dc level at IC2.

To implement this approach, the output of VFIC1 is differentiated by IC4, an op-amp connected as a high gain differentiator. The output is non-zero with any a.c. signal at VFIC1.

The output of IC4 is then digitized by an analog-to-digital conversion, yielding a logic high if and only if there is no A.C. signal from IC1. If a high is maintained for 300 msec., a 2 msec one-shot pulse turns on switch IC8 through a voltage interface circuit. Switch IC8 shorts R2 with 1200 ohms. The time constant of the switch resistance and C1 is now;

$$RC = (1200 \text{ ohms})\ (24 \text{ ufd}) = 0.00288 \text{ sec.}$$

Three time constants, necessary for 95% settling, are now only 8.64 msec rather than two hours.

The falling edge of the 2-msec pulse triggers a 5 msec pulse. The end of the 5 msec pulse retriggers the 2 msec pulse as long as no A.C. signal is present from IC1. Thus R2 is shorted by 1200 ohms for 2 msec out of 5 msec as long as no A.C. signal is present.

Should a 2 msec pulse occur just as a signal appears at the input of IC1, the following calculations yield the amount of error introduced.

a) assume a truck velocity of 70 mph

b) assume 40-foot bridge span

c) assume full-scale signal of 1.0 volt

d) assume a linear ramp signal for convenient calculations.

e) $$t_{span} = \frac{40 \text{ ft) } (3600 \frac{\text{sec}}{\text{hr}})}{(70 \frac{\text{mile}}{\text{hr}}) \text{ (5280 ft/mile)}} = 0.390 \text{ sec.}$$

f) $V_{error} \simeq \Delta V_{sig}$ in 2 msec.

$$\Delta V_{sig} = \frac{V_{sig}}{\frac{1}{2} t_{span}} \times t_{pulse}$$

$$= \frac{1.0 \text{ volt}}{(0.5)\ (.390)} \times 0.002 = 0.010 \text{ volt}$$

This 10 mvolt error, should it occur, is within accuracy specifications.

Assume the polarity switch is in the (+) position and V_{sig} is positive going (Fig. 3-5).

As V_{sig} rises above the threshold set by R1001, the comparator goes high, setting the S-R latch high, which

triggers a 40-msec one-shot pulse. The pulse turns on the impact counter, via a driver, long enough to ensure a count.

The S-R latch stays high, holding the counter disabled, until V_{sig} returns to near zero. As V_{sig} drops to less than $+ V_{ref}$ of the +R reset comparator, the output of the +R reset buss goes high, resetting the S-R latch and reenabling the counter circuit. Thus only one count is ensured per signal per channel.

The polarity switch allows monitoring of either positive or negative going signals. Operation for negative going signals involves switching the polarity of the threshold voltage, inverting the now complemented output of the counter comparator, and resetting the S-R latch with the -R reset buss. The latch and one-shot driver now function the same as for positive-going signals.

3.3 THE POWER SUPPLY

The instrument may be powered by any direct current power source which satisfies the following requirements: system voltage - 24 VDC (nominal); strain transducer - 38 milliamperes; recorder - 6 milliamperes. Since both the output of the strain transducer and the triggering voltages are directly proportional to the power supply voltage, the instrument will function normally under power supp;y fluctuations from 28 volts DC to 20 volts DC.

The system has been tested with a power supply consisting of two 12-volt automobile batteries rated at 95 ampere hours. At 70°F this battery pack will supply enough power for instrument operation up to approximately 80 days between

recharges. Although this is quite an economical power supply which provides for long periods of operation, the size of the batteries requires a separate battery case. The 55-pound weight of each of these batteries also makes them rather difficult to handle in the field.

A second alternative power supply consists of two 12-volt motorcycle batteries rated at 11 ampere hours. These batteries are much smaller and lighter than the automobile batteries and can be enclosed in the same protective cover as the recorder. At 70°F these batteries must be recharged every six or seven days.

A third alternative power supply consists of four Ever-ready No. 1461 Hot Shot Dry Cell batteries. These batteries can also be enclosed in the same protective cover with the recorder and they are not subject to acid spillage which can be a problem with the wet cell batteries. At 70°F a set of these batteries will power the instrument for approximately fifteen days. Although this is probably the most convenient of the three power supplies, it is also the most expensive because the batteries are not rechargeable.

A 12 volt rechargeable dry cell intended for portable TV sets has been introduced since the power supply testing phase of the project. Although these batteries have not been tested it appears that two of them would power the unit for one to two weeks between recharges. Manufacturers literature indicates that they can be recharged 30 or 40 times. If tests prove this information to be correct these batteries will provide the most convenient and economical power supply of all.

3.4 TOTAL INSTRUMENT PACKAGE

The transducer, recorder and power supply (except in the case where automobile batteries are used) all fit inside a tamper-proof enclosure, 48 x 18 x 9 inches. Both the transducer and tamper-proof enclosure are clamped to the bottom flange of the steel girder with screws located inside the enclosure. No special surface preparation is required for the transducer.

Basic resolution of the electronic counter circuits is plus or minus ten millivolts (75 psi for steel). However, triggering levels for counters must be separated by at least 20 millivolts (150 psi for steel). Linearity of the differential transformer is 0.5% (maximum error = 37.5 psi for steel) and its resolution is theoretically infinite. The calibration factor for the differential transformer varies 4 or 5 percent between transformers. Therefore, the precision of the instrument is dependent on the effort put into matching the recorder circuit to the transducer. However, a one or two percent match is not difficult.

Although a precise definition of the overall accuracy of the instrument would be quite complex, it is reasonable to assume that for the majority of data collected on steel bridges actual triggering levels will be within plus or minus

150 psi of the value set.

A parts list and circuit diagrams are present in Appendices B and C. It is estimated that at the present time the cost of constructing additional units would be approximately $3500 each.

CHAPTER 4

DATA ANALYSIS

4.1 EXAMPLE OF FATIGUE ANALYSIS

Data and procedures presented in this report will now be used to illustrate a relatively simple approach for performing a fatigue analysis. A numerical example has been given previously (Chapter 2) for the determination of the desired stress ranges and the cumulative exceedences associated with each range. To avoid redundancy, the data given in Figure 2-9 will be used directly as shown in Figure 4-1.

1. Plot stress range vs. cumulative exceedences as shown in Figure 4-1. Extrapolate this curve by any convenient method to obtain an intersection with the abscissa (in this example, from a straight line extrapolation through 9.0 ksi, the intersection is found to be 9.3 ksi. For convenience, 9.5 ksi will be used).

2. Determine fatigue life at each stress range as given in column 4 of Table 4-1.

3. Compute damage/cycle, number of cycles, and total damage for each interval as shown in columns 5, 6, and 7, respectively, in Table 4-1.

4. Compute Σ total damage from column 7.

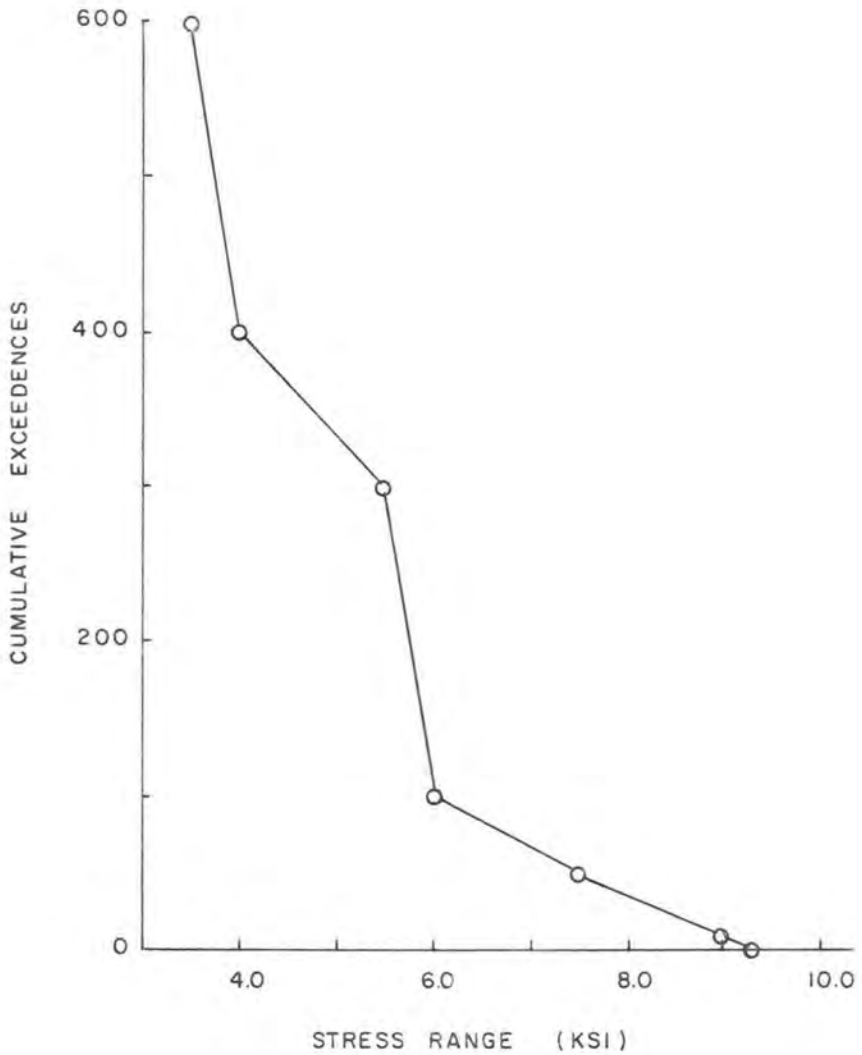

FIGURE 4-1 CUMULATIVE EXCEEDENCE CURVE FOR SAMPLE EXTRAPOLATION.

Table 4-1

Sample Calculations for Fatigue Analysis

i	Stress Range (ksi) Sr_i	Cum. Exceed. Cr_i	Fatigue Life $\times 10^6$ N_i	Damage / Cycle $\times 10^{-6}$ $\frac{1}{2}(\frac{1}{N_i}+\frac{1}{N_{i+1}})$	Cycles A_i $(Cr_{i+1}-Cr_i)$	Total Damage $\times 10^{-6}$ $\frac{A_i}{2}(\frac{1}{N_i}+\frac{1}{N_{i+1}})$
(1)	(2)	(3)	(4)	(5)	(6)	(7)
Upper Bound	9.5	0	1.45			
				0.639	10	6.39
1	9.0	10	1.70			
				0.504	40	20.16
2	7.5	50	2.38			
				0.336	50	16.80
3	6.0	100	3.97			
				0.184	200	36.80
4	5.5	300	8.70			
				0.0915	100	9.15
5	4.0	400	14.7			
				0.0512	200	10.24
6	3.5	600	29.1			

Σ TOTAL DAMAGE $= 99.54 \times 10^{-6}$

Assuming that the test period in this example is 24 hours, the total annual damage is given by

$$\text{annual damage} = (99.54 \times 10^{-6}) \times 365$$
$$= 0.0363$$

Since from Miner's theory (Chapter 2) failure occurs when the total damage is equal to unity, the fatigue life, on the basis of the data above, is calculated as

$$\text{fatigue life} = 1.0/\text{annual damage}$$
$$= 1.0/0.0363 = 28 \text{ years}$$

The fatigue life calculated above should be considered as the theoretical expected life under present conditions. Traffic volume increases, changes in legal weight limits, and improper maintenance resulting in corrosion may all serve to reduce the life of a bridge significantly.

4.2 CRITICAL STRESSES

Although there is usually only one location of maximum stress in any given bridge span, it may be of interest to obtain stress histories at various connection details where stress concentrations are likely to occur. In addition, certain sections in multi-span bridges may experience maximum stresses that are relatively small but, due to stress reversals, their resultant stress range may be significant. Therefore, it may be desirable to measure, or at least estimate, the stress levels occurring at any or all of these points.

Results of this study indicate that the transducer may be located at some conveniently accessible point on a bridge girder and, by the use of influence envelopes, the recorded stresses may be projected to obtain a reasonable estimate of the stresses that occur at other desired points. The accuracy of the projected estimate is dependent on parameters which will be discussed in Section 4.3.

4.3 INFLUENCE ENVELOPES FOR MULTI-SPAN BRIDGES

In general, the strain transducer should be located at, or as close as practicable to, the point at which a stress or strain history is desired. However, for the purpose of estimating stresses at points away from the strain transducer, it is proposed that maximum moment envelopes may be used, within limitations, to project recorded data from one point to another.

In order to obtain a maximum moment envelope for a bridge, it is necessary to consider some vehicle moving across the bridge with the gross weight of the vehicle distributed to discrete points according to the axle spacing. The maximum moment envelope then represents the maximum positive and negative moments, at each point along the structure, resulting from the passage of the vehicle. Such an envelope actually indicates the maximum moment range that occurs at any given point. From the maximum moment range envelope, a maximum stress range envelope may be obtained directly by considering the section properties at each point.

For composite bridges, however, the appropriate section properties must be considered independently for the positive and negative bending moments before obtaining the stress range envelope. With respect to a fatigue analysis the maximum stress range envelope provides a desirable representation of data. For ease in usage, the stress range envelope may be normalized at any given point by setting the stress range at that point equal to unity and adjusting the remaining stress ranges accordingly. This normalized envelope is quite useful in observing the relative difference between the stress range at a given point and the stress range at the point of normalization. Furthermore, if the strain transducer is located at the point of normalization then the recorded stress ranges may be projected to another point by multiplying by the appropriate ordinate on the normalized envelope.

It is obvious that a wide variety of axle spacing and axle weight distribution combinations are possible. To consider all such combinations for each individual bridge would be prohibitive from a practical standpoint; however, in preceding experimental analyses (6, 7, 8, 9) several common truck types have been classified according to gross weight, axle spacing, and axle weight distribution.

In this study, three truck types (Figure 4-2) have been considered. In particular, Type I and Type II correspond to two types classified by Galambos, et al. (7) as 3 and 2S-1, respectively. These two types were selected to

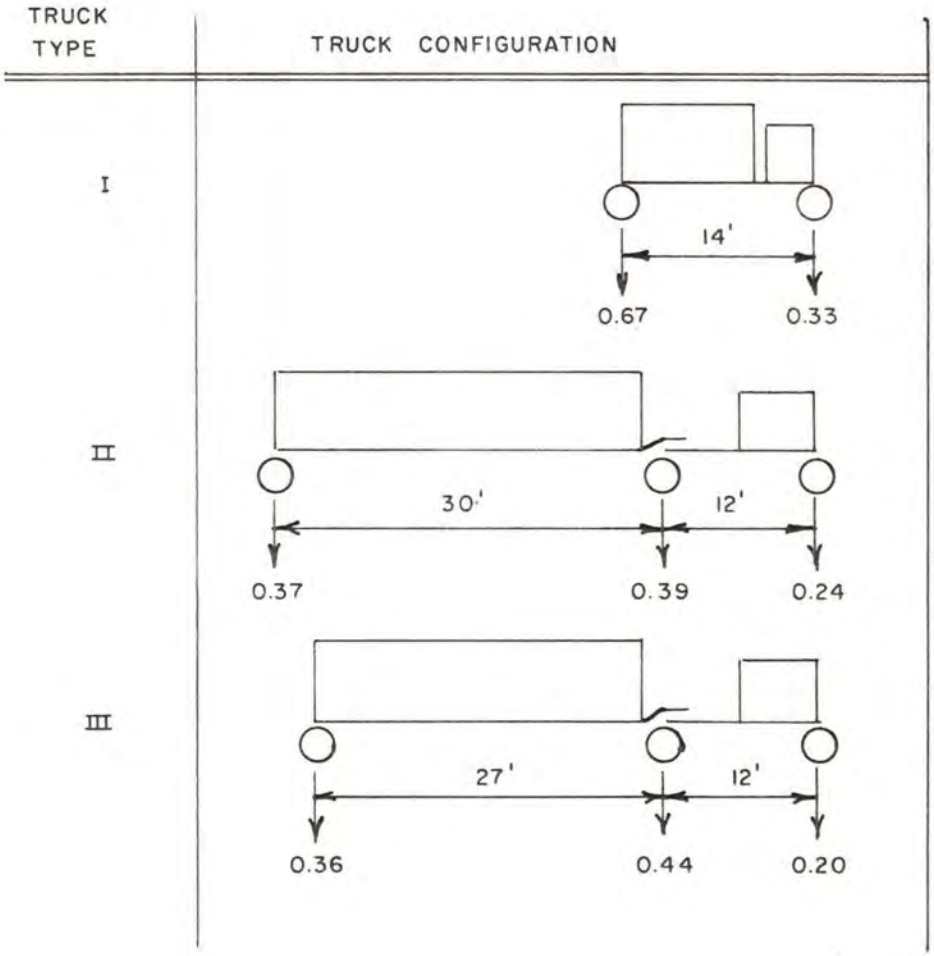

FIGURE 4-2 AXLE SPACING AND WEIGHT DISTRIBUTION FOR TRUCK TYPES I, II AND III.

provide a maximum variation in the relative curvature of their normalized moment envelopes. The Type III truck was proportioned to produce a median normalized moment envelope from which variations in relative curvatures can be observed.

As an example, consider the three-span continuous bridge profile shown in Figure 4-3. The span ratios and section properties were selected as being representative of a typical highway bridge. For computations the following bridge properties have been assumed:

non-composite deck

total length = 99.0 ft.

depth of beam section = 24"

cover plate thickness = ½"

I (cover plate section) = 1.5 I (beam section)

The maximum moment envelopes for truck types I, II and III were obtained, using ICES STRUDL II.[1] From these envelopes the corresponding stress-range envelopes were obtained, using the section properties from above. These stress-range envelopes were then normalized about the section of maximum moment and are shown in Figure 4-4.

It is important to note that the bandwidths, at points near the point at which the envelopes are normalized, are relatively small. Specifically, maximum variations from the Type III truck, up to 6/10 of the span length approximately (+6% to -2%) in this example. Subsequent variations

---

[1]Computerized structural design language - ICES STRUDL II - has the capability to determine maximum moment envelopes directly from a given set of loading conditions.

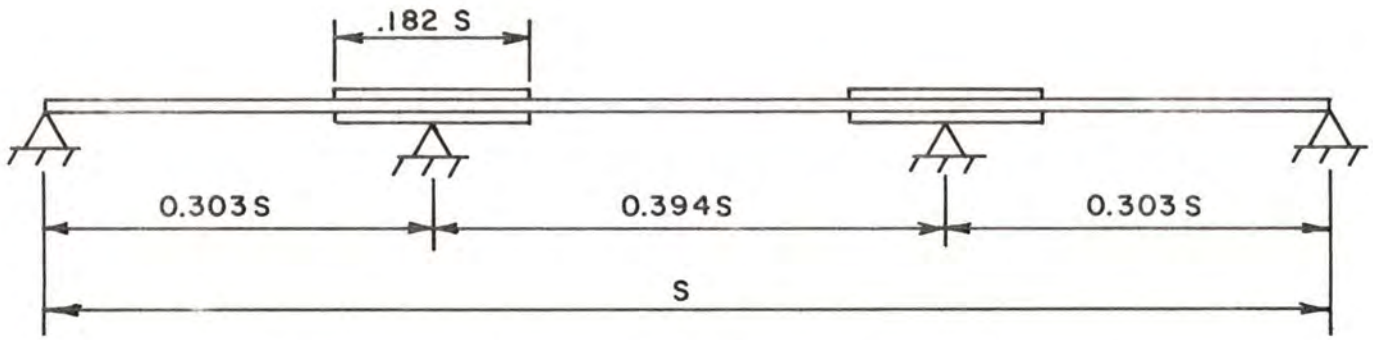

I_C (COVER PLATE SECTION) = 1.5 I_B (BEAM SECTION)

FIGURE 4-3 THREE SPAN CONTINUOUS BRIDGE PROFILE.

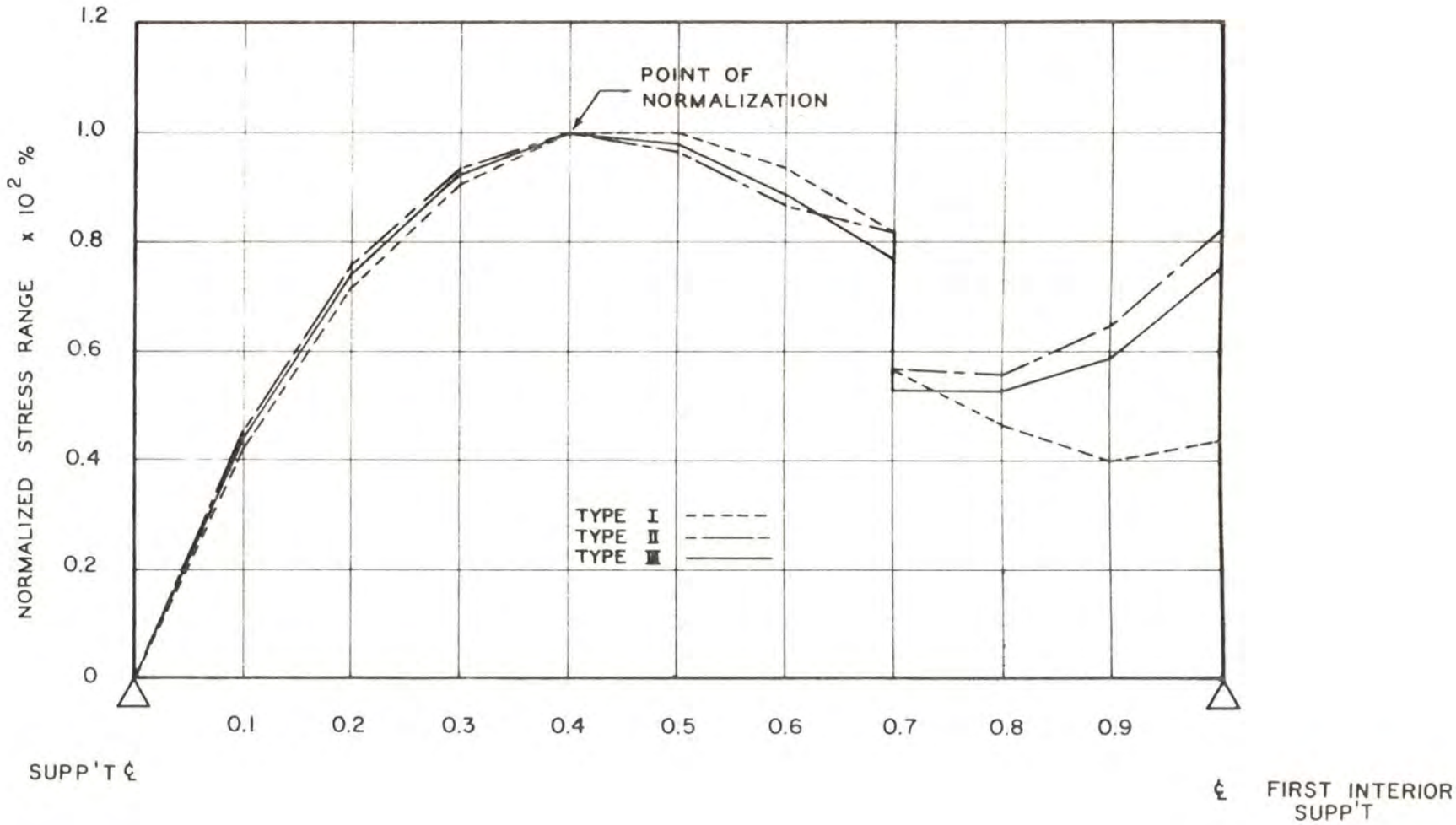

FIGURE 4-4 MAXIMUM STRESS RANGE ENVELOPE FOR SAMPLE 3-SPAN BRIDGE
(LEFT END SPAN)

become quite large (+7% to -43%) at the first interior support.

While variations near the point of normalization are small, the stress-range envelopes for generally all truck types should fall within the extremes of Types I and II. From this it is apparent that a composite truck similar to Type III can, in general, be used to represent the overall truck population as long as the inherent errors in doing so are recognized. In addition, it is important to note that it is necessary to compute maximum moment ordinates only at points where stress ranges are desired. Therefore, if only a small number of points are to be considered, then it may not be desirable to compute a complete maximum moment envelope.

In summary, it is worthy of mention, once again, that the accuracy obtained using this technique of stress projection is highly dependent on the variations observed in the family of maximum moment envelopes to be considered as well as the distance from the strain transducer to the point at which stresses are to be projected. Furthermore, it should be recalled that the stress-range envelopes presented in this section are based on a total bridge length of 99.0 feet. For longer bridges, the variation in relative curvature of such envelopes should be expected to decrease with the ratios of axle spacing to span length. In addition, studies have been conducted (14, 15) to investigate the variations between the static and dynamic responses of highway bridges. These

studies indicate that the dynamic response may result in fluctuations of the maximum moment envelope; however, an impact study conducted by Baldwin (16) for a 3-span continuous bridge has shown that dynamic stress oscillations generally follow the shape of an influence line for stress. Thus the general curvature of the maximum moment envelope should not be changed significantly if the amplitude of the dynamic stress oscillations is relatively small in comparison to the static stresses caused by the same load. It is therefore concluded that the dynamic response of a highway bridge will not effect the usage of the proposed instrumentation as long as the basic limitations, described previously, are considered.

CHAPTER 5

INSTALLATION AND OPERATION

5.1 GENERAL

Although the self-monitoring instrument has been designed to provide simplicity of installation, operation, and data analysis, optimum results require that the user familiarize himself with the particular bridge before field installation of the instrument. This familiarization should include determination of the critical sections to be studied, maximum and minimum expected stress levels, and traffic volume. Also note that the strain transducer measures the average strain over the 40" gage length. Therefore, any changes in section properties of the girder within the gage length should be accounted for.

In addition to the instrument, an attempt has been made to provide a weatherproof and tamper-proof enclosure. It is still desirable to locate the instrument in as inconspicuous and protected a spot as possible. The following step-by-step procedure is suggested for installation of the instrument components.

5.2 INSTALLATION OF COMPONENTS

5.2.1 The Strain Transducer and Housing Assembly

1. Determine location of desired stresses.

2. Attach transducer mounting blocks (Fig. 5-1A). The transducer mounting blocks are attached to a spacer bar for ease of carrying. The bar also automatically locates the blocks at the specified 40" gage length. One point should be marked 20" on either side of the desired stress point and the mounting blocks attached at those points
   a. Tighten mounting screws a and b (Fig. 5-1B) at least 1/2 turn past finger tight.
   b. Tighten mounting screws c and d finger tight only.
3. Remove spacer bar.

5.2.2 <u>The Recorder Housing Assembly</u>

1. Position recorder housing assembly (Fig. 5-2) as near as possible on the left of the transducer housing. Each end of the housing is clamped to the bottom flange by two allen screws located on top of the flange and inside the housing (Fig. 5.3)
2. Set instrument rack in place (Fig. 5-4).
3. Set recorder in place (Fig. 5-5).
4. Install Batteries (Fig. 5-6).
5. Connect Cables (Fig. 5-7).

FIGURE 5-IA STRAIN TRANSDUCER WITH SPACER BAR

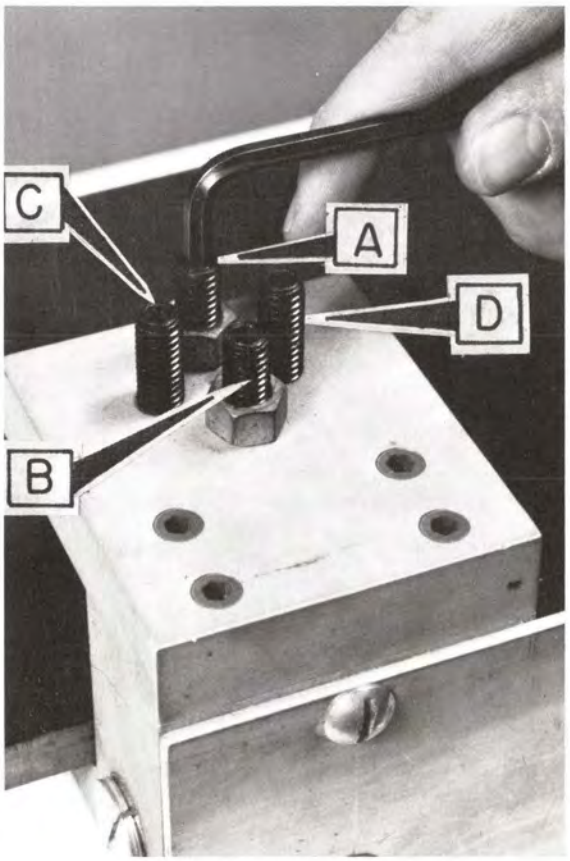

FIGURE 5-IB TRANSDUCER MOUNTING BLOCK

FIGURE 5-2 RECORDER HOUSING ASSEMBLY

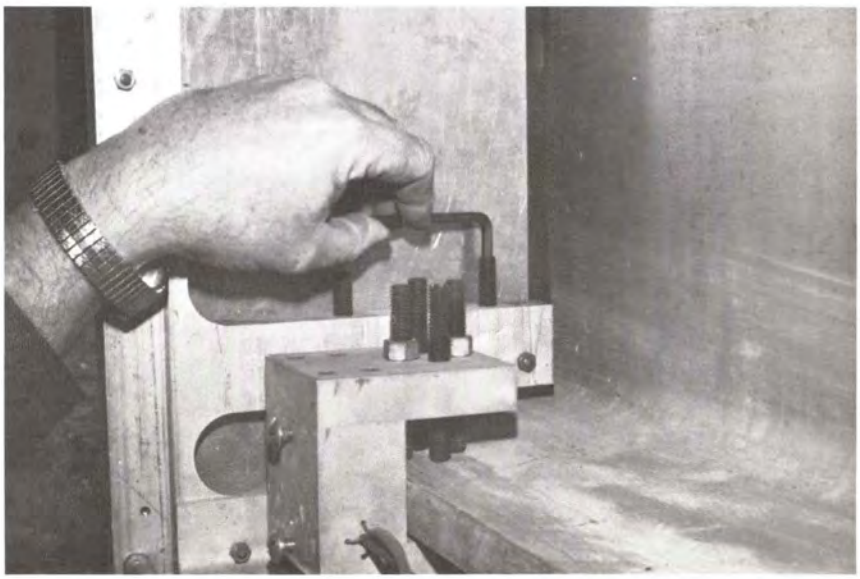

FIGURE 5-3 RECORDER HOUSING CLAMPING SCREWS

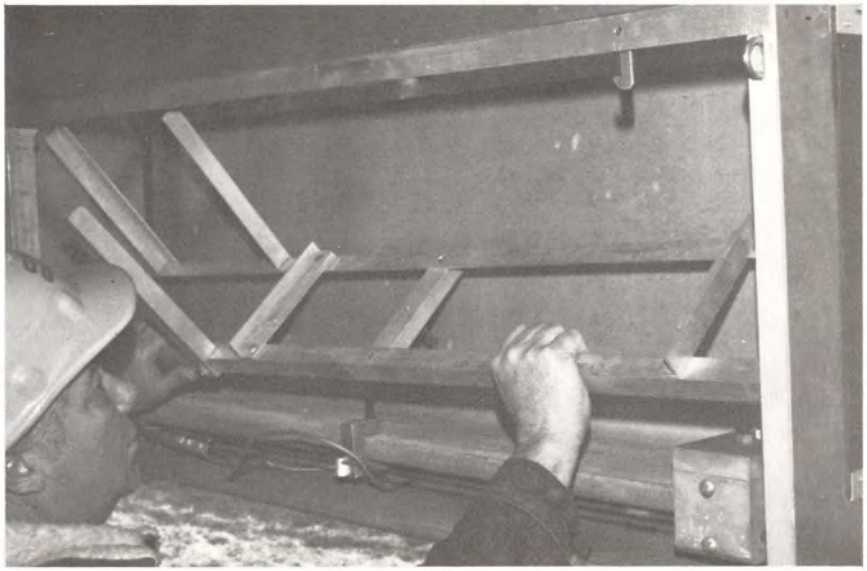

FIGURE 5-4 INSTRUMENT RACK

FIGURE 5-5 POSITIONING RECORDER

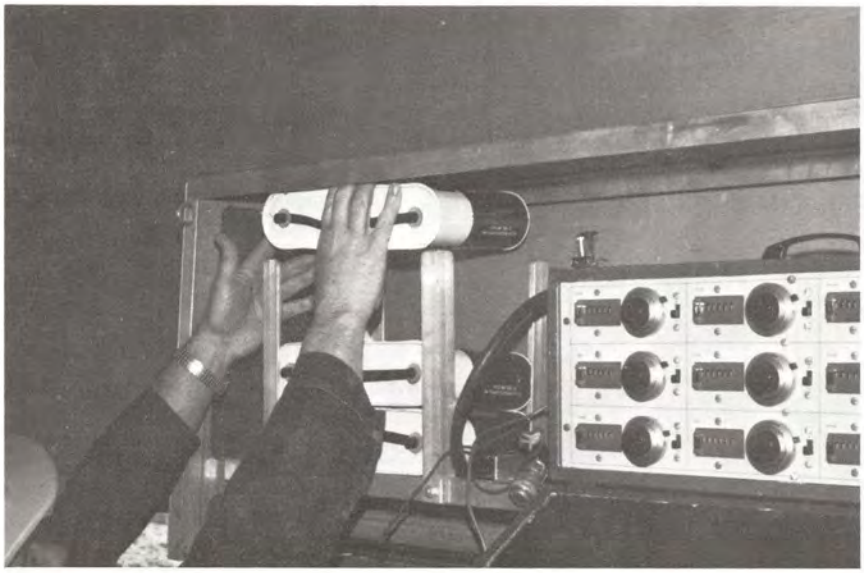

FIGURE 5-6 INSTALLING BATTERIES

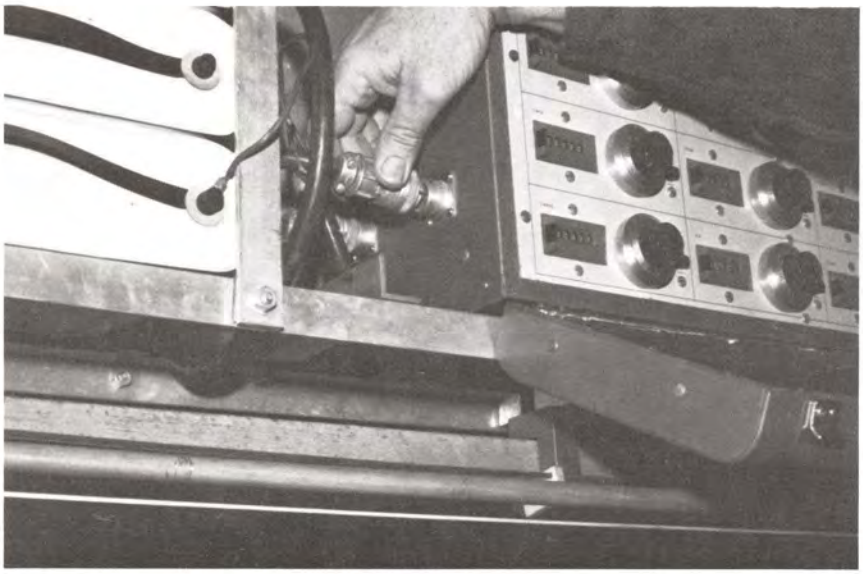

FIGURE 5-7 CABLE CONNECTION

5.3 INSTRUMENT OPERATION

After installation of the system components is complete, turn switch on to apply power to the transducer and recorder and make the following operational adjustments.

1. Set strain transducer to zero with the zero adjustment (Fig. 5-8A) using a portable voltmeter (Fig. 5-8B). The strain transducer need only be set approximately to zero in order to be within the linear operating range of the DCDT. Slight errors will be compensated by drift circuitry.
2. Set appropriate counter triggering levels (Fig. 5-9A) and zero counters by pushing reset buttons (Fig. 5-9B). A positive or negative stress level is selected by a switch adjacent to each potentiometer. Each division on the precision potentiometers represents 1 millivolt or a stress of 7.5 psi. Thus for a stress level of 1000 psi the potentiometer should be set to

$$\frac{1000}{7.5} = 133$$

3. Close and lock all protective covers. (Fig. 5-10)

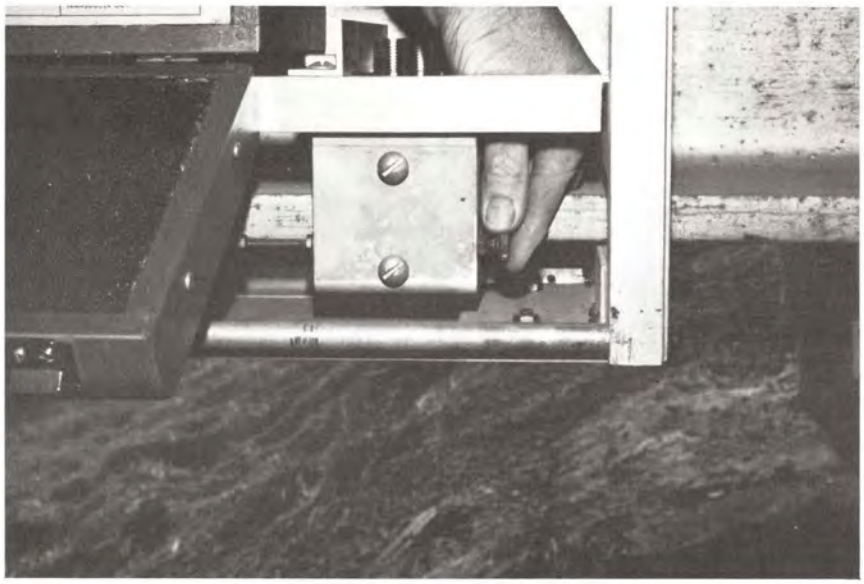

FIGURE 5-8A TRANSDUCER ZERO ADJUSTMENT

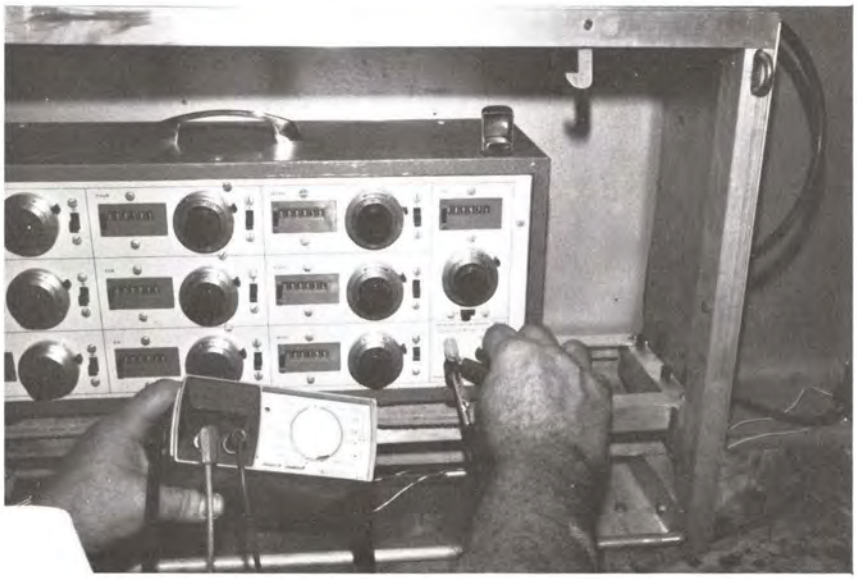

FIGURE 5-8B CHECKING TRANSDUCER ZERO

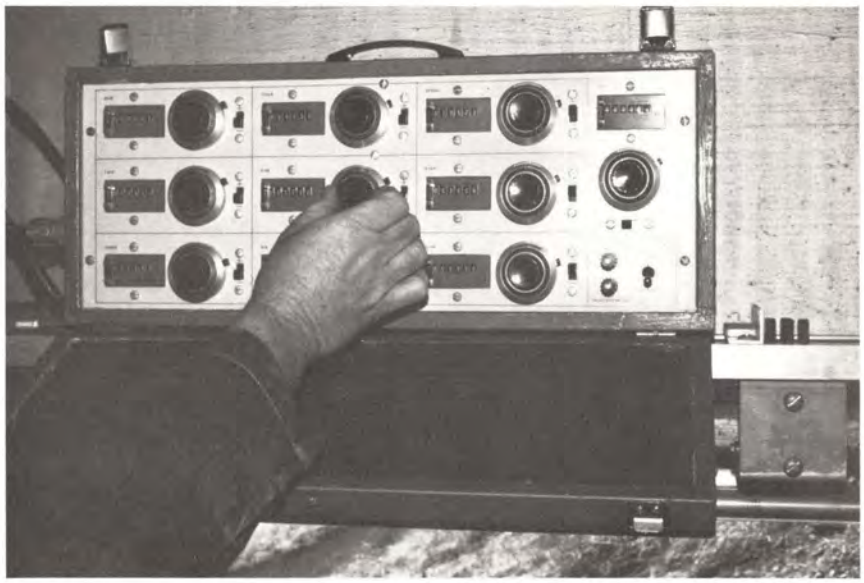

FIGURE 5-9A SETTING TRIGGERING LEVELS

FIGURE 5-9B RESETING COUNTER

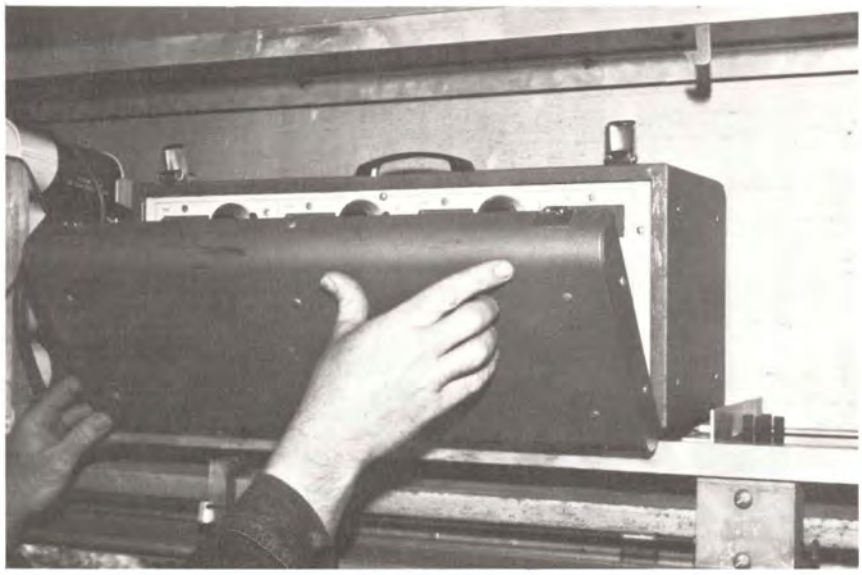

FIGURE 5-10A WATERPROOF RECORDER COVER

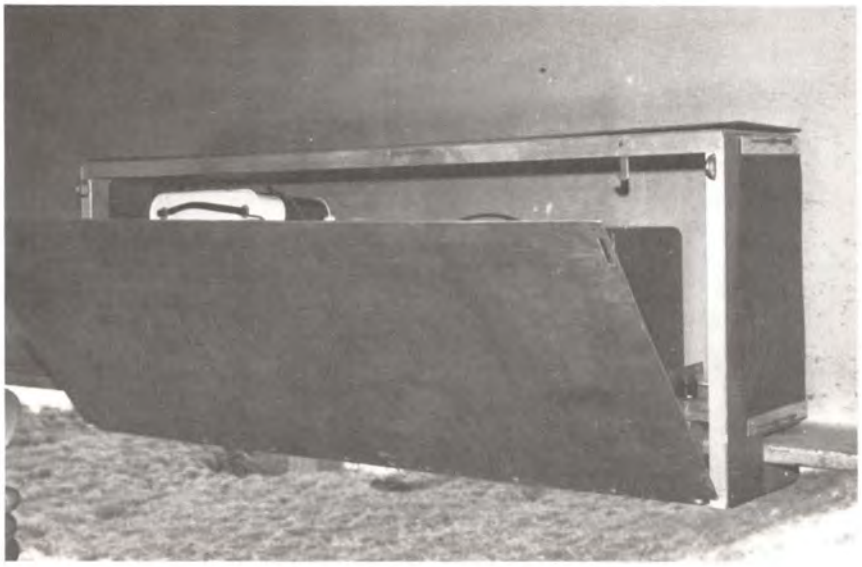

FIGURE 5-10B HOUSING COVER

The system is now ready for operation. For the purpose of data analysis, an accurate record should be kept of the number of hours the instrument is in operation.

CHAPTER 6

Field Test

6.1 STRUCTURE

The instrument was field tested on the bridge carrying the west bound lanes of Interstate 70 across Perchy Creek just west of Columbia, Missouri. There are a total of 9 spans in the bridge and the west 3 spans are a continuous structure with details shown in Figure 6-1. Stresses were recorded on the bottom flange of the first interior girder on the right hand side in the west end span of the bridge. A section 24 feet in from the end of the bridge was selected for the measurement because the maximum positive moment should occur very close to this section.

6.2 RECORDING OF DATA

On the afternoon of December 4, 1975, the instrument was installed (Fig. 6-2) with a new set of 6 volt dry cell batteries. Initial battery voltage was 25.3 volts. Preliminary observations during the month of November had indicated the approximate maximum stress ranges and the potentiometeres were set at the values shown in Table 6-1. At 3:30 p.m. all counters were set to zero and the tamper-proof enclosure was locked.

During the following two weeks the recorder was checked periodically to see that it was still operating and at 2:20 p.m. on December 19 the counter readings shown in Table 6-1 were

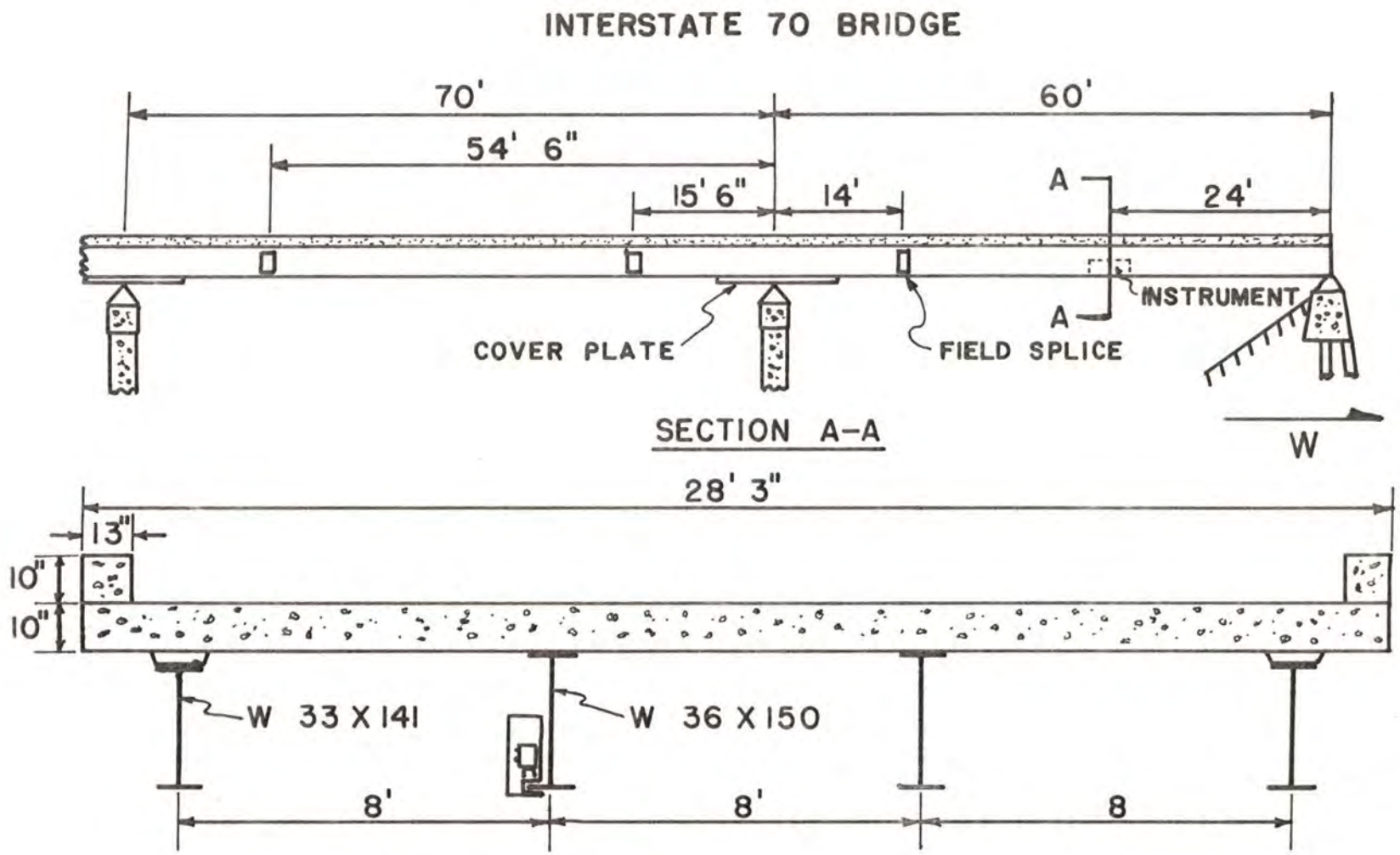

FIGURE 6-1 FIELD TEST LAYOUT

FIGURE 6-2 FIELD INSTALLATION

TABLE 6.1

STRESS HISTORY

Dec. 4 - Dec. 19

COUNTER NO	POTENTIOMETER SETTING	TRIGGER STRESS	COUNTS	STRESS RANGE	NO. OF EXCEEDENCES
1	67	500	25291	750	25291
2	133	1000	16246	1250	16246
3	200	1500	9875	1750	9875
4	267	2000	4700	2250	4700
5	333	2500	228	3250	228
6	400	3000	17	3750	17
7	-33	-250	39172	250	39172
8	-67	-500	4570	2500	4500
9	-100	-750	283	2750	283
10	-233	-1750	0		

TABLE 6.2

STRESS HISTORY

Dec. 19 - Dec. 31

COUNTER NO.	POTENTIOMETER SETTING	TRIGGER STRESS	COUNTS	STRESS RANGE	NO. OF EXCEEDENCES
1	67	500	13309	750	13309
2	133	1000	8321	1250	8321
3	200	1500	4968	1750	4968
4	267	2000	2472	2250	2472
5	333	2500	128	3000	128
6	400	3000	3	4000	3
7	-33	-250	19571	250	19571
8	-67	-500	2005	2500	2005
9	-100	-750	58	3250	58
10	-133	-1000	4	3500	4

recorded. At that time, the battery voltage had dropped to 18 volts but the recorder was still operating normally.

The data indicated that the triggering level for counter number 10 should be reset to a lower value, but triggering levels for all other counters were set properly. A new set of batteries was installed and the initial voltage measured at 25.3 volts. With potentiometers set at the values shown in Table 6-2, the counters were reset to zero at 2:50 p.m., December 19, and the tamper-proof enclosure was again locked.

At 2:10 p.m., December 31, counter readings were recorded as shown in Table 6-2. Counters were still functioning normally and the battery voltage had dropped to 19.2 volts. A drift of 117 milivolts in the transducer zero position was observed. However, the drift compensation circuitry was properly accounting for this drift because all counters were resetting after the passage of each vehicle and the balance between positive and negative counts was the same as when the recorder was first installed.

6.3 ANALYSIS OF DATA

Determination of stress ranges and the number of times each was exceeded are shown in Tables 6-1 and 6-2 for the two test periods respectively. Since these stress ranges were all below the normally accepted threshold for fatigue damage in base metal, no cumulative damage calculations were made. However, plots of cumulative stress range exceedances and stress histograms are shown in Figures 6-3 and 6-4 for the two test periods respectively.

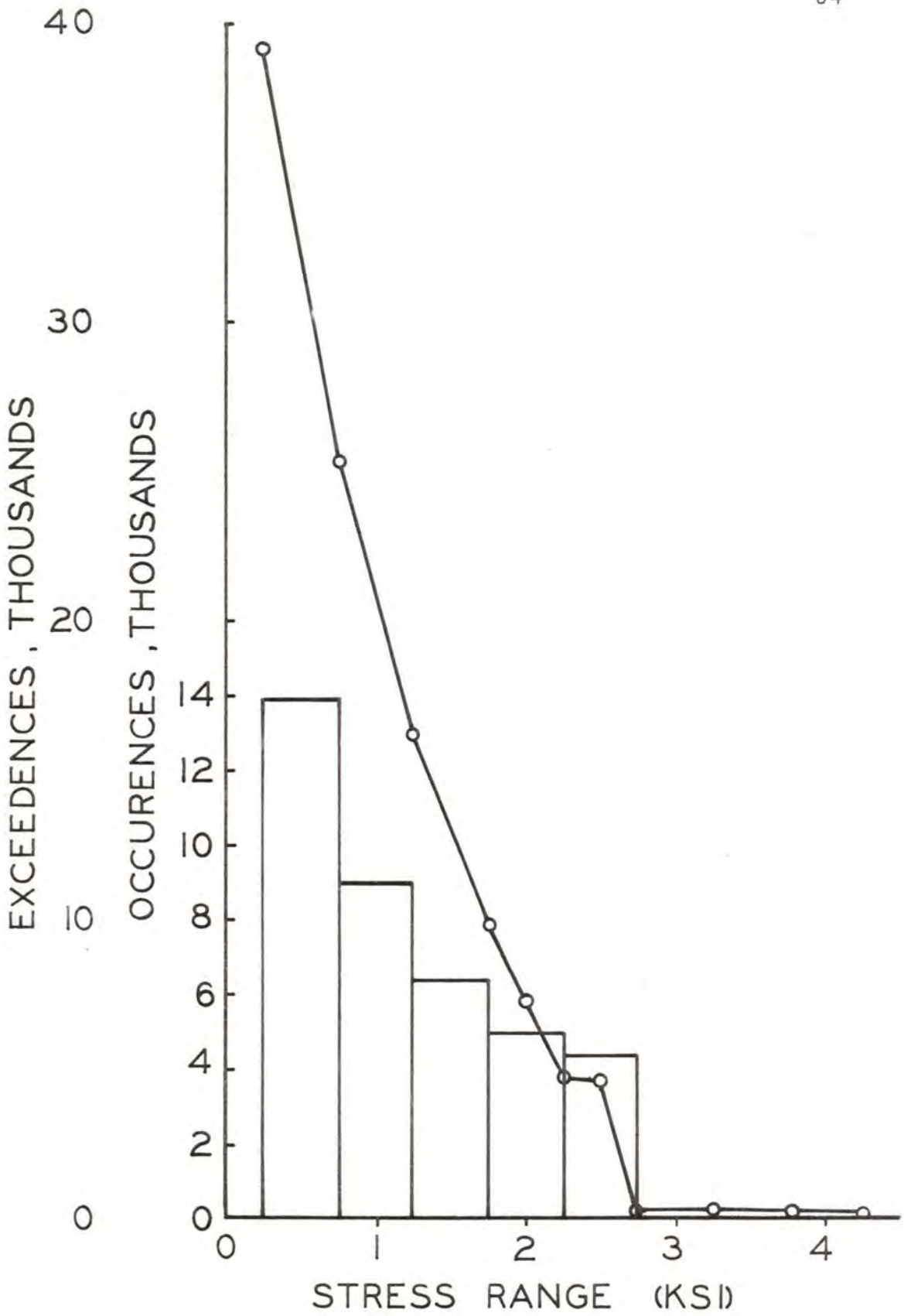

FIGURE 6-3 STRESS RANGES
DEC. 4-19

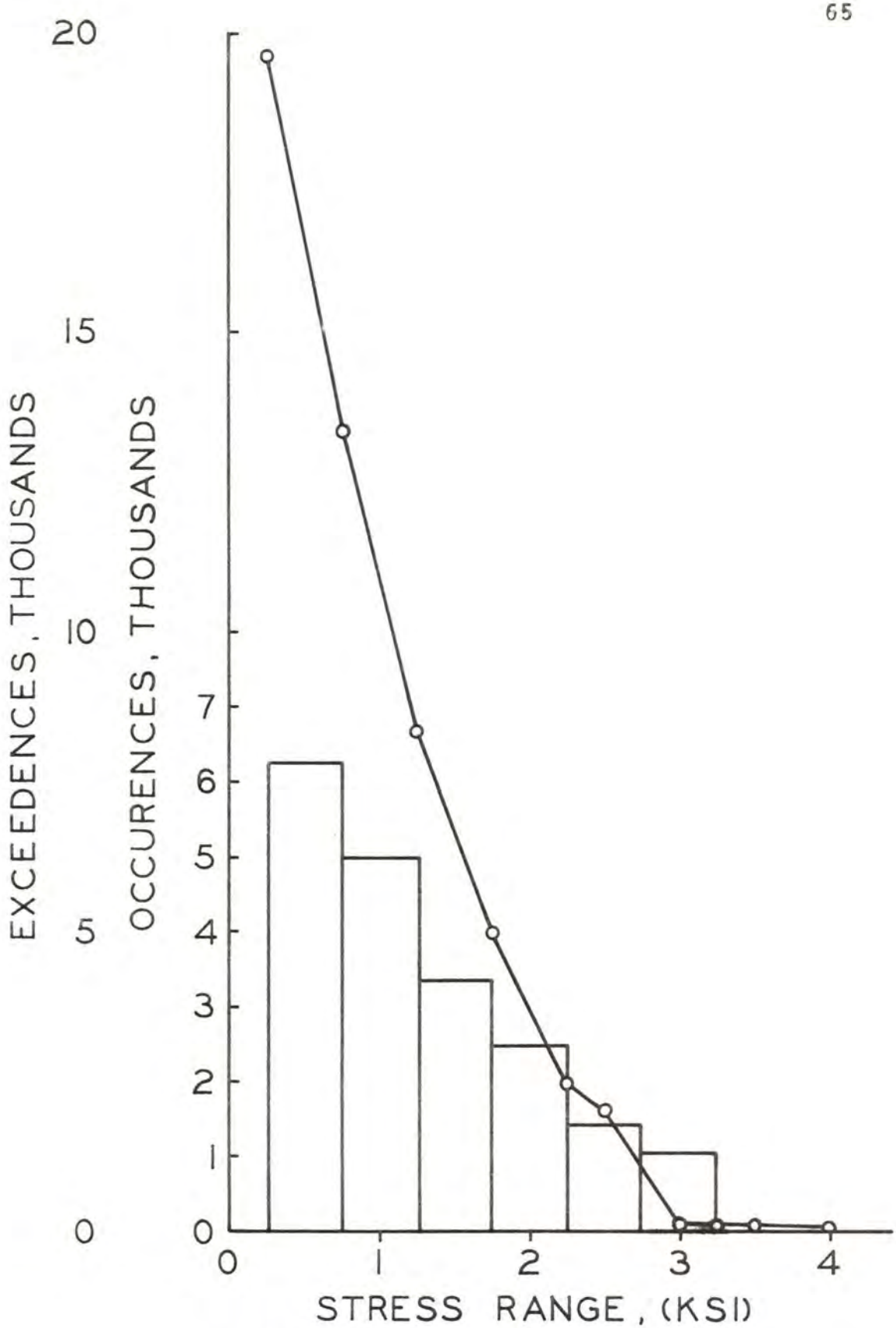

FIGURE 6-4 STRESS RANGES
DEC. 19-31

Data for the period December 19 - 31, indicates only half as much truck traffic as was indicated for a similar period earlier in the month. This reflects the reduced truck traffic over the Christmas and New Years holidays and is in agreement with observations of the Highway Patrol at their weigh stations.

The instrument seems to work very well under field conditions with battery life very close to that projected from laboratory tests. Field installation was easy and could be performed by one man. However, a second man is quite helpful and greatly reduces the number of trips up and down the ladder.

CHAPTER 7

SUMMARY

The self-monitoring instrument for load history studies is presented here as an economical means for collecting data that reflects the actual service stresses occurring in a structural steel highway bridge. In addition, the availability of the instrument will make possible the collection of load history data from a wider variety of bridges for much longer periods of time than may be obtained using present techniques.

The complete system consists of: (1) the strain transducer, (2) the recorder, and (3) the battery pack. System design is such that the instrumentation may be attached to a structural steel bridge girder and left in place for extended periods of time subject only to battery recharging at intervals of approximately 6-80 days, depending on the battery pack used. Furthermore, simplified data analysis techniques are presented which allow accumulated data to be used directly to obtain results in terms of a stress-range-frequency histogram or in terms of bridge fatigue life. In addition, procedures have been developed for the purpose of estimating stress ranges at points other than the location of the strain transducer. Application of these techniques and procedures may be expected to yield suitable accuracy and were developed for

ease in understanding and usage by personnel having only a fundamental knowledge of fatigue and bridge behavior.

Finally, step-by-step installation and operation procedures are provided for ease in application of the instrumentation.

Field tests show that the instrument works well under field conditions. Installation requires approximately 20 minutes while batteries can be replaced and a set of readings taken in about 5 minutes.

LIST OF REFERENCES

1. Bowers, D. G., "Loading History, Span #10, Yellow Mill Pond Bridge, I-95, Bridgeport, Connecticut," HPR 175-332, Connecticut Department of Transportation, Jan. 1973.

2. Munse, W. H., Lenzen, K. H., Yen, B., Nordmark, G. E., Yao, J., "Analysis and Interpretation of Fatigue Data," Jour. Struct. Div., Proc. ASCE, Vol. 74, No. ST12, Proc. Paper 6283, Dec. 1968.

3. Goodpasture, D. W., Burdette, E. G., "A Comparison of Bridge Stress History Results With Design Related Analyses," University of Tennessee, Jan. 1973.

4. Christiano, P. P., Goodman, L. E., Sun, C. N., "Bridge Stress Range History," Highway Research Record, No. 382, 1972.

5. Douglas, T. R., "Fatigue Life of Bridges Under Repeated Highway Loading," Highway Research Record, No. 382, 1972.

6. Heins, C. P., Khosa, R. L., "Comparison Between Induced Girder Stresses and Corresponding Vehicle Weights," Highway Research Record, No. 382, 1972.

7. Galambos, C. F., McKeel, W. T., Maddox, C. E., Kinnier, H. L., "Loading History of Two Highway Bridges in Virginia," Highway Research Record, No. 382, 1972.

8. Cudney, G. R., "Stress Histories of Highway Bridges," Jour. Struct. Div., Proc. ASCE, Vol. 94, No. ST12, Proc. Paper 6289, Dec. 1968.

9. Galambos, C. F., Armstrong, W. L., "Acquisition of Loading History Data on Highway Bridges," Public Roads, Vol. 35, No. 8, June, 1969.

10. Galambos, C. F., Heins, C. P., "Loading History of Highway Bridges, Comparisons of Stress Range Histograms," Highway Research Record, No. 354, 1971.

11. Miner, M. A., "Cumulative Damage in Fatigue," Journal of Applied Mechanics, Vol. 12, No. 1, Sept. 1945.

12. Munse, W. H., Stallmeyer, J. E., "Fatigue in Welded Beams and Girders," Highway Research Board, Bulletin 315, 1962.

13. Fisher, J. W., Frank, K. H., Hirt, M. A., McNamee, B. M., "Effect of Weldments on the Fatigue Strength of Steel Beams," NCHRP, Report 102, HRB Washington, D.C., 1970.

14. Veletsos, A. S., Fenves, S. J., Seiss, C. P., "Dynamic Studies of the AASHO Road Test Bridges," Special Report 71, NAS-NRC, Washington, D.C., 1962.

15. Walker, W. H., "Dynamic Stresses and Deflections in Highway Bridges," 16th Annual Structural Engineering Conference, University of Kansas, Lawrence, April 1971, and 12th Annual Bridge Engineering Conference, Colorado State University, Fort Collins, April 1971.

16. Baldwin, J. W., Jr., "Impact Study of a Steel I-Beam Highway Bridge," University of Missouri-Columbia, Engineering Experiment Station Series, No. 58, 1964.

APPENDIX A

NOMENCLATURE

APPENDIX A

NOMENCLATURE

A_i = The total number of cycles occurring in the stress range interval, $Sr_{i+1} < Sr_i$.

C_1 = The reading on counter #1 indicating the cumulative number of exceedences of the positive threshold level, which also corresponds to the total number of significant events over a given test period.

C_i = The reading on counter i indicating the cumulative number of exceedences of stress level σ_i.

C_j = The reading on counter j indicating the cumulative number of exceedences of a particular negative stress level σ_j.

Cr_i = The cumulative number of exceedences of stress range Sr_i.

m = The number of active counters.

n_i = The actual number of cycles incurred at a given stress range.

N_i = The number of cycles to failure at a given stress range.

σ_i = The stress level at which C_i is incremented.

σ_j = A particular negative stress level at which C_j is incremented.

Sr_i = Stress range; defined as the algebraic difference between the maximum and minimum stress values for each loading cycle.

APPENDIX B

PARTS LIST

APPENDIX B

ELECTRICAL PARTS LIST FOR RECORDER

P/N	Description
	Capacitors
C1A	12 ufd, film 200v
C1B	12 ufd, film 200v
C2	12 ufd, film 200v
C3	0.1 ufd, 50-v Mylar
C4	0.1 ufd, 50-v Mylar
C5	0.22 ufd, 50-v Mylar
C6	0.0047 ufd, 50-v Mylar
C7	0.0033 ufd, 50-v Mylar
C101	100 ufd, 35v electrolytic
C102	100 ufd, 35v electrolytic
C103	0.1 ufd, 50-v Mylar
C104	0.1 ufd, 50-v Mylar
C105	1000 ufd, 35-v electrolytic
C201	0.1 ufd, 50-v Mylar
C201	0.1 ufd, 50-v Mylar
C202	0.1 ufd, 50-v Mylar
CX001	0.068 ufd, 50-v Cer.
	Counters
LX001	Rowan 6-Digit Manual Reset Counter
	Diodes
D1	1N4148, signal
D101	1N4001, rectifier
D102	1N4001, rectifier
ZD1	T1754A, 6.2v. Zener
ZD2	T1754A, 6.2v Zener
ZDX001	TI 747A, 3.2v Zener

Integrated Circuits

IC1	AD511B, Analog Devices FET-Input Op-Amp
IC2	AD511B, Analog Devices FET-Input Op-Amp
IC3	LM4250, National Semi. Programmable Op-Amp.
IC4	LM4250, National Semi. Programmable Op-Amp.
IC5	LM2390, National Semi. Quad Comparator
IC6	CD4001, RCA Quad NOR, CMOS
IC7	CD4001, RCA Quad NOR, CMOS
IC8	CD4016, RCA Quad Analog Switch
IC9	LM210D, Nat. Semi. Voltage Follower
IC10	LM4250, Nat. Semi. Programmable Op-Amp.
IC11	LM4250, Nat. Semi. Programmable Op-Amp.
IC12	LM4250, Nat. Semi. Programmable Op-Amp.
IC13	LM4250, Nat. Semi. Programmable Op-Amp.
IC14	LM4250, Nat. Semi. Programmable Op-Amp.
IC15	LM4250, Nat. Semi. Programmable Op-Amp.
IC16	LM239D, Quad Comparator, Nat. Semi.
IC17	CD4009, Hex Inverter, RCA
IC18	CD4001, Quad NOR Gate, RCA
IC19	CD4001, Quad NOR Gate, RCA
IC20	CD4009, Hex Inverter, RCA
IC21	CD4001, Quad NOR Gate, RCA
IC22	LM239D, Quad Comparator, Nat. Semi.
IC23	CD4009, Hex Inverter, RCA
IC24	CD4001, Quad. NOR Gate, RCA
IC25	CD4001, Quad NOR Gate, RCA
IC26	CD4009, Hex Inverter, RCA
IC27	CD4001, Quad. NOR Gate, RCA
IC28	LM239D, Quad. Comparator, Nat. Semi.
IC29	CD4009, Hex Inverter, RCA
IC30	CD4001, Quad. NOR Gate, RCA

Printed Circuits

P.C.1	Custom, By IDG, UMC, 14"x5.5", 792 holes, D.S.

Resistors

R1	10MΩ, 10% 1/4-w, carb. comp.
R2	50MΩ, 1% 1/2-w, wire-wound
R3	84, 5KΩ, 1%, 1/4-w, met. film
R4	73.2 KΩ, 1% 1/4-w, met. film
R5	20KΩ, Variable
R6	84.5KΩ, 1%, 1/4-w, met. film
R7	73.2KΩ, 1%, 1/4-w, met. film
R8	20KΩ, 10%, Variable
R9	20MΩ, 10% 1/4-w, carb. comp.
R10	10KΩ, 10%, 1/4-w, carb. comp.
R11	2.2MΩ, 10%, 1/4-w, carb. comp.
R12	2.2MΩ, 10%, 1/4-w, carb. comp.
R13	100KΩ, 10%, 1/4-w, carb. comp.
R14	1MΩ,
R15	3.3KΩ,
R16	1MΩ, 10%, 1/4-w, carb. comp.
R17	3.3KΩ, 10%, 1/4-w, carb. comp.
R18	1MΩ.
R19	2MΩ,
R20	1MΩ,
R21	1MΩ,
R22	2.2MΩ,
R23	1MΩ,
R24	1MΩ,
R25	1MΩ,
R26	100KΩ,
R101	100KΩ,
R102	25KΩ, 10%, variable
R103	100KΩ, 10%, 1/4w, carb. comp.
R104	56KΩ,
R105	180KΩ,

	Resistors (Cont'd)
R106	56KΩ,
R107	100KΩ,
R108	10KΩ, 10% Variable
R109	100KΩ,
R110	10KΩ, 10%, Variable
R111	100Ω, 10%, 1/4-w, carb. comp.
R201	1MΩ,
R202	2KΩ,
R203	20MΩ,
R204	10KΩ,
R205	100KΩ,
R206	1MΩ,
R207	2KΩ,
R208	20MΩ,
R209	10KΩ,
R210	100KΩ, 10%, 1/4-w, carb. comp.
RX001	100KΩ, .1%, precision 10-turn pot.
RX002	1MΩ, 10%, 1/4-w, carb. comp.
RX003	750KΩ, 10%, 1/4-w, carb. comp.
RX004	10KΩ, 10%, 1/4-w, carb. comp.
	Switches
SW1	PPDT, power (micro) switch, 10A @ 250 voc.
SWX001	TPDT, slide switch, 3A @ 125 vac.
	Transistors
Q1	MPS-A14, NPN Darlington, Motorola
Q201	MPS-A14, NPN Darlington, Motorola
Q202	MPS-A14, NPN Darlington, Motorola
QX001	MPS-A14, NPN Darlington, Motorola

Wiring Harness Color Codes

Color	Signal
blue	+1v.d.c.
black	-1 v.d.c.
yellow	+R
Purple	-R
Orange	$+C_x$
brown	$-C_x$
white	S_x
black	R_z

Single wires are coded to their channel number.

Color	Signal
brown	Channel 1
red	2
orange	3
yellow	4
green	5
blue	6
purple	7
brown/green	8
white	9
black	10

+1v.d.c., -1v.d.c., +R, -R are bussed to the polarity switches.

$+C_x$, $-C_x$, S_x, R_x are bundled with V_x from each channel.

K_x is harnessed separately to provide noise isolation.

APPENDIX C

CIRCUIT DIAGRAMS

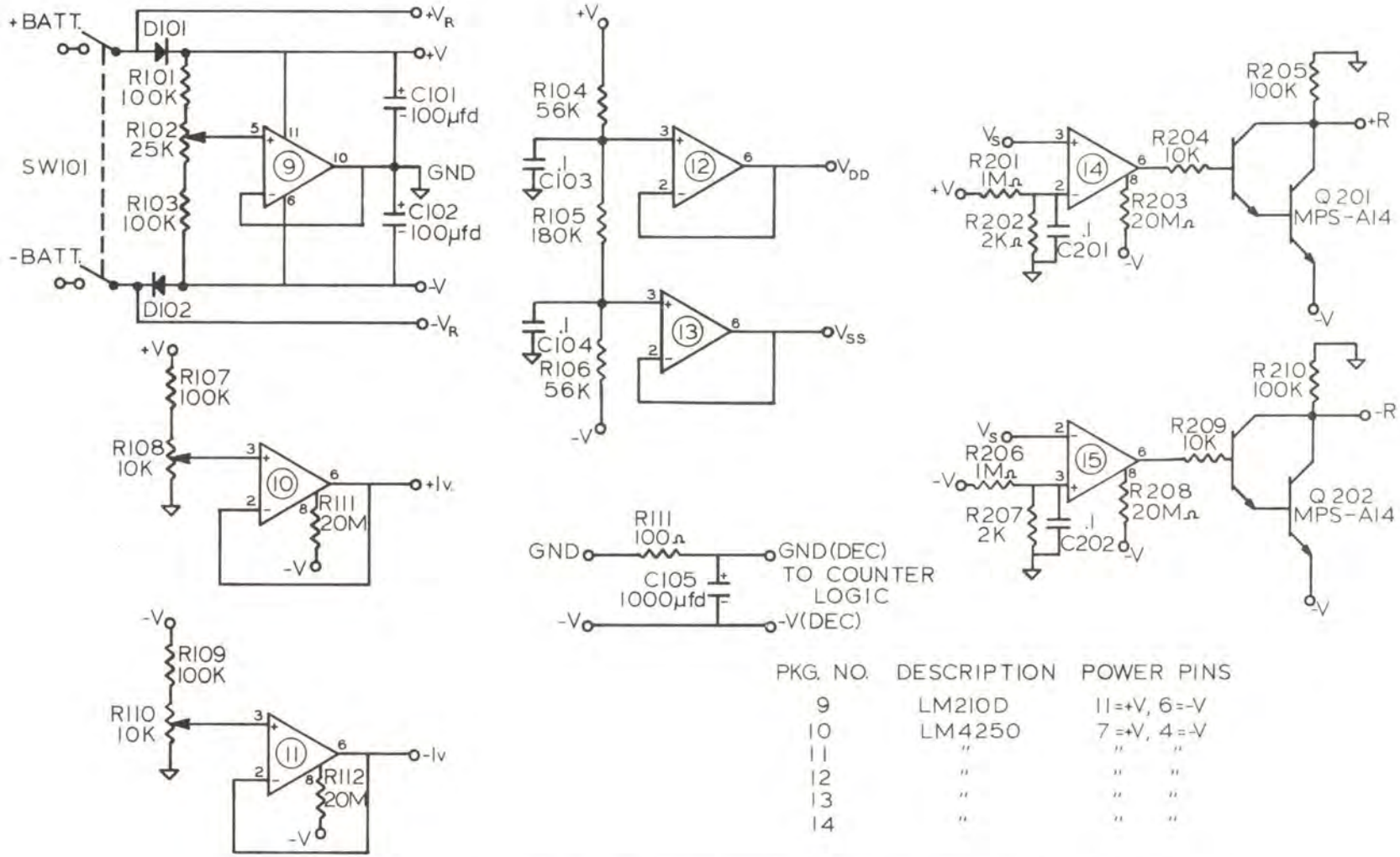

PKG. NO.	DESCRIPTION	POWER PINS
9	LM210D	11=+V, 6=-V
10	LM4250	7=+V, 4=-V
11	"	" "
12	"	" "
13	"	" "
14	"	" "

C-1 POWER SUPPLIES & RESET BUSSES

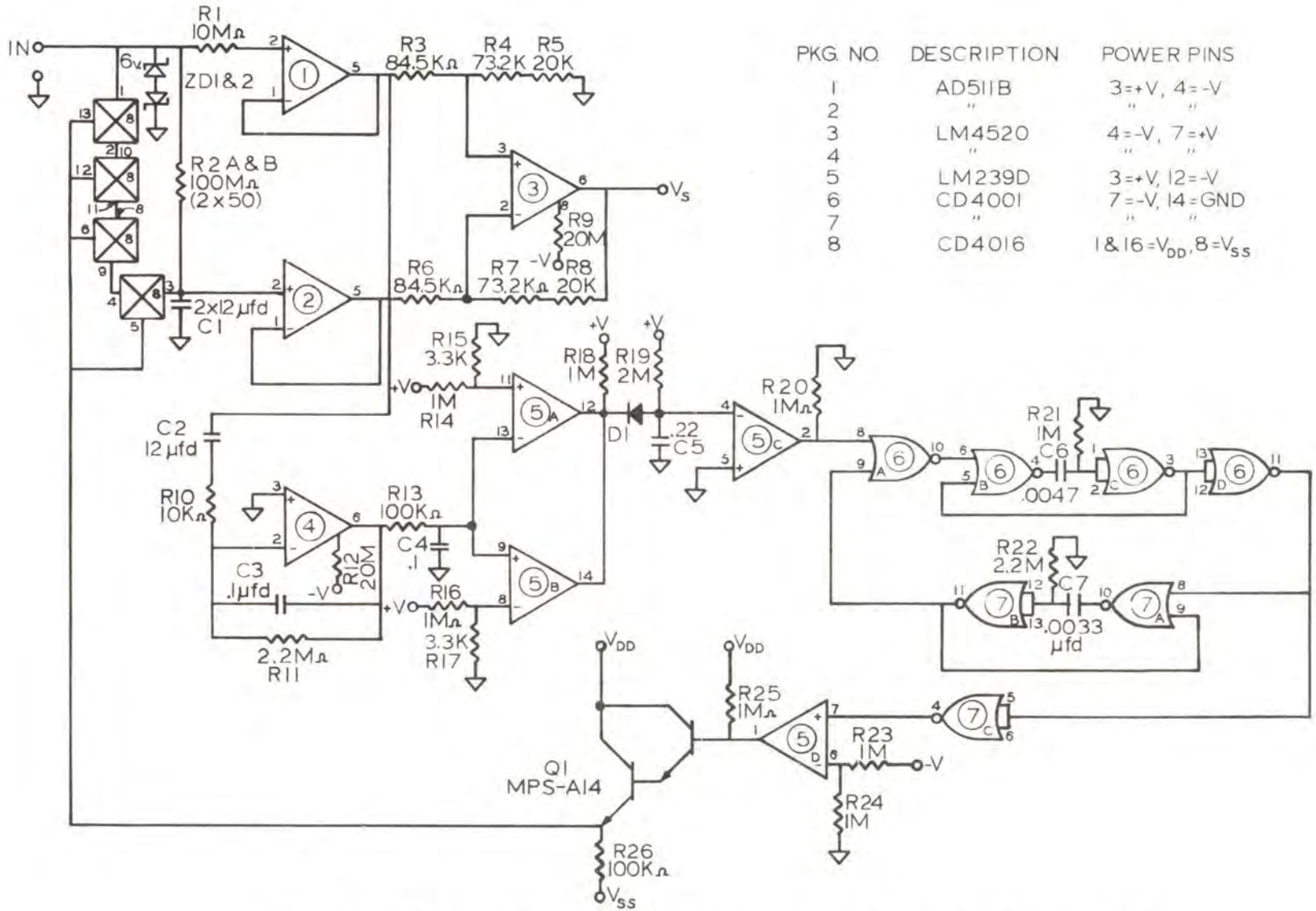

PKG. NO.	DESCRIPTION	POWER PINS
1	AD511B	3=+V, 4=-V
2	"	" "
3	LM4520	4=-V, 7=+V
4	"	" "
5	LM239D	3=+V, 12=-V
6	CD4001	7=-V, 14=GND
7	"	" "
8	CD4016	1&16=V_{DD}, 8=V_{SS}

C-2 TRANSDUCER SIGNAL CONDITIONING

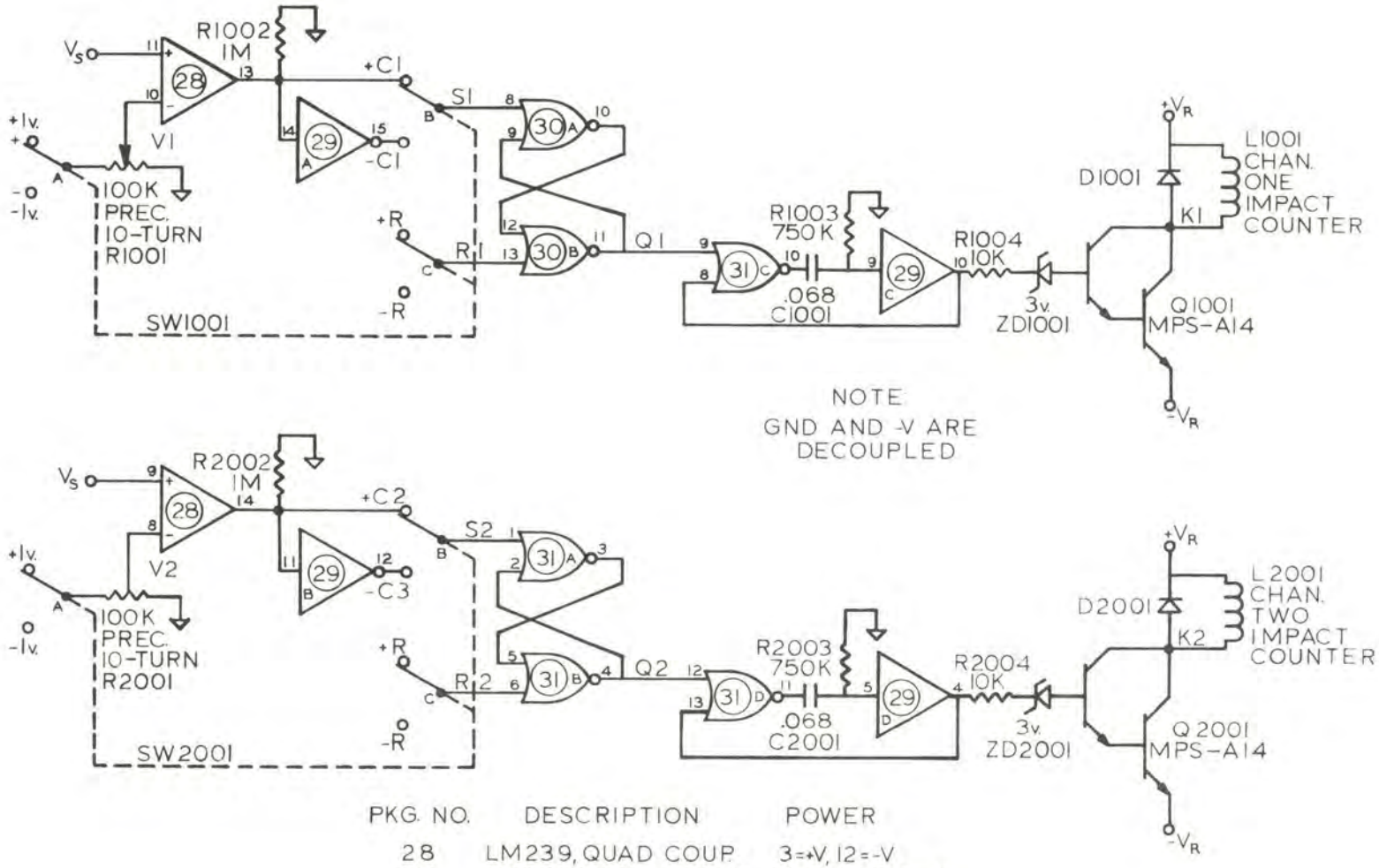

PKG. NO.	DESCRIPTION	POWER
28	LM239, QUAD COUP.	3=+V, 12=-V
29	CD4009, HEX INVERT	1&16=GND, 8=-V
30	CD4001, QUAD NOR	14=GND, 7=-V
31	" "	" "

C-3 CHANNELS ONE & TWO

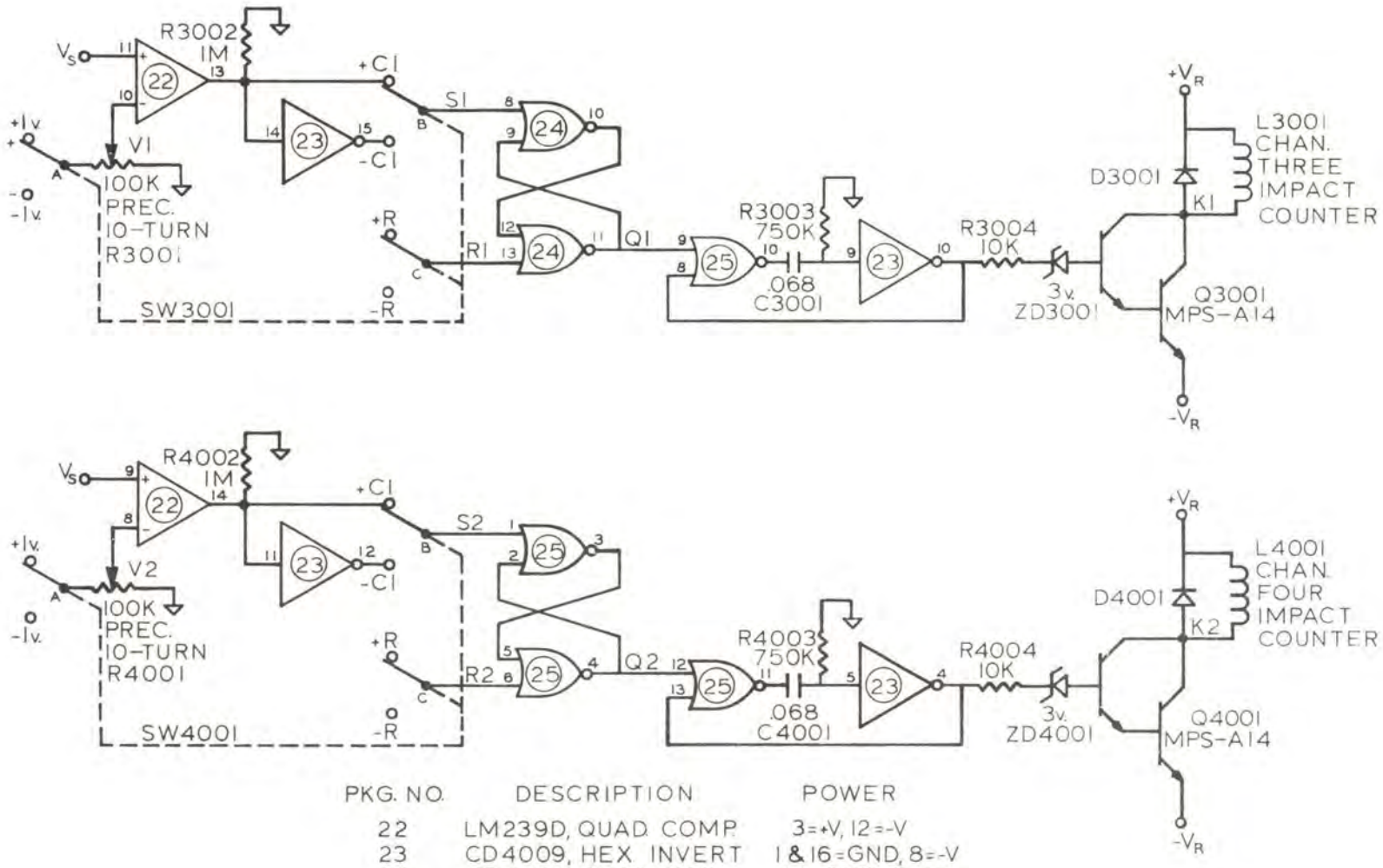

PKG. NO.	DESCRIPTION	POWER
22	LM239D, QUAD COMP.	3=+V, 12=-V
23	CD4009, HEX INVERT	1 & 16=GND, 8=-V
24	CD4001, QUAD NOR	14=GND, 7=-V
25	" "	" "

C-4 CHANNELS THREE & FOUR

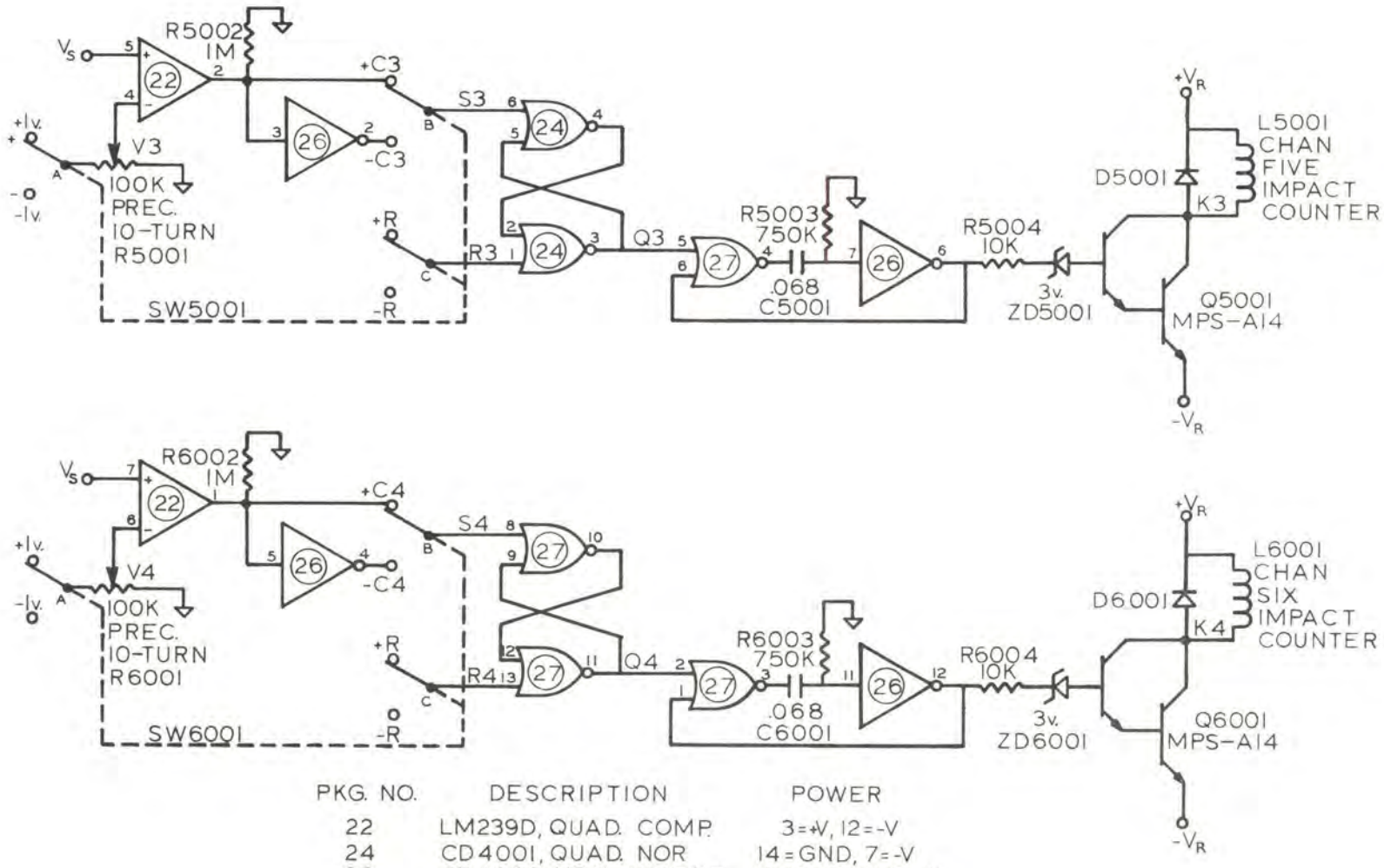

PKG. NO.	DESCRIPTION	POWER
22	LM239D, QUAD. COMP.	3=+V, 12=-V
24	CD4001, QUAD. NOR	14=GND, 7=-V
26	CD4009, HEX INVERT.	1 & 16=GND, 8=-V
27	CD4001, QUAD. NOR	14=GND, 7=-V

C-5 CHANNELS FIVE & SIX

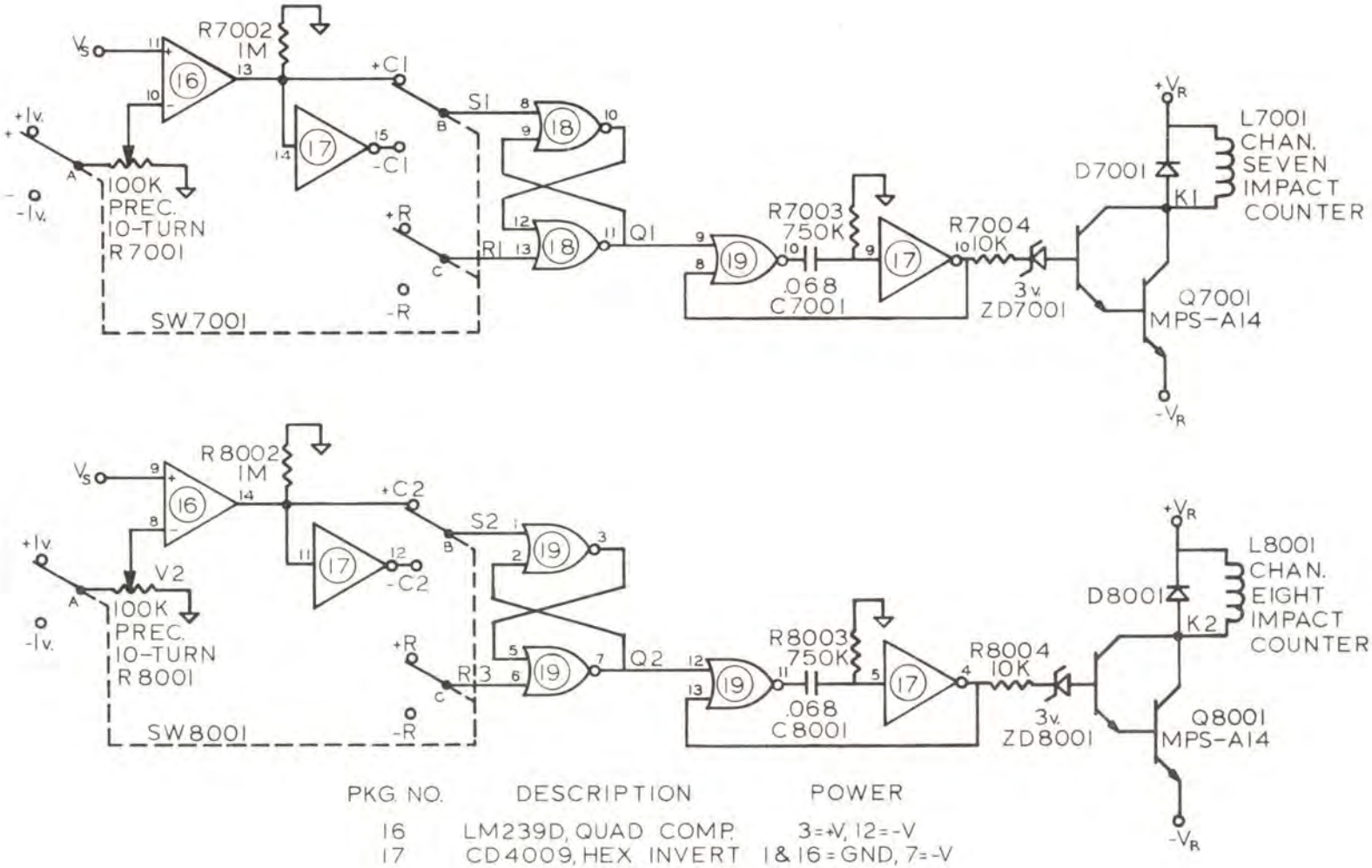

PKG. NO.	DESCRIPTION	POWER
16	LM239D, QUAD COMP.	3=+V, 12=-V
17	CD4009, HEX INVERT	1 & 16 = GND, 7=-V
18	CD4001, QUAD. NOR	16 = GND, 7=-V
19	" "	" "

C-6 CHANNELS SEVEN & EIGHT

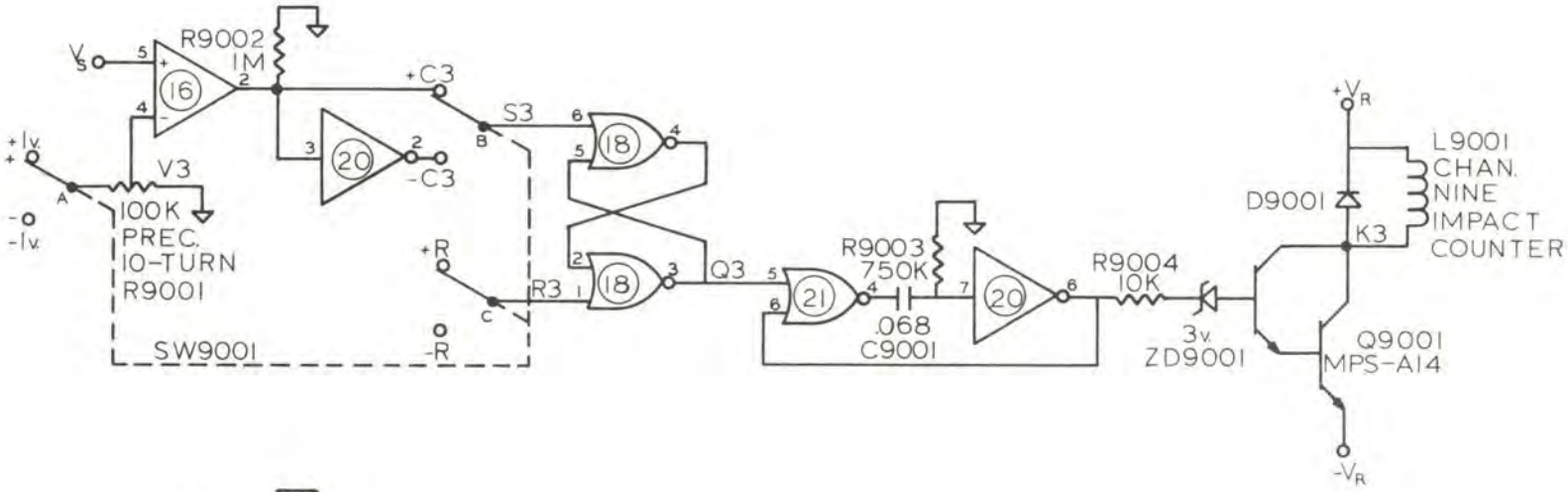

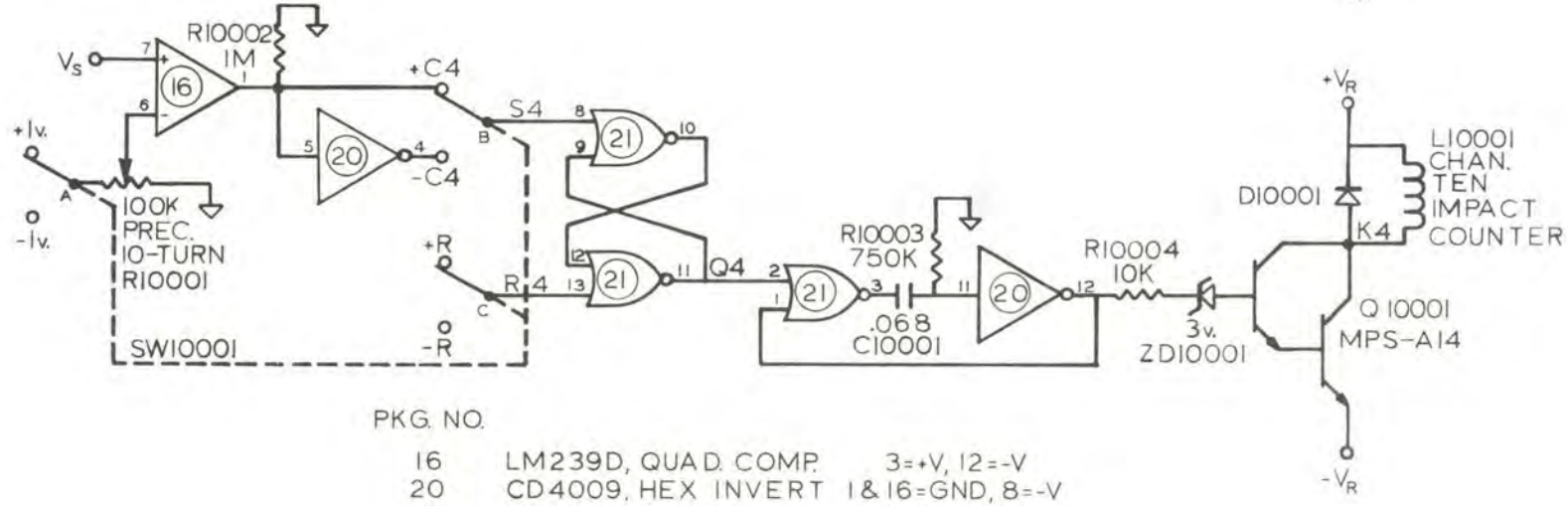

PKG. NO.		
16	LM239D, QUAD. COMP.	3=+V, 12=-V
20	CD4009, HEX INVERT	1 & 16=GND, 8=-V
18	CD4001, QUAD NOR	14=GND, 7=-V
21	" "	" "

C-7 CHANNELS NINE & TEN

MoDOT Library
RD0015765